5th INTERNATIONAL MAAR CONFERENCE

Maars associated with fracture- and/or conduit-controlled aquifers in folded limestone in San Luis Potosí, México

Pre-conference Field trip
5th International Maar Conference, Querétaro, México

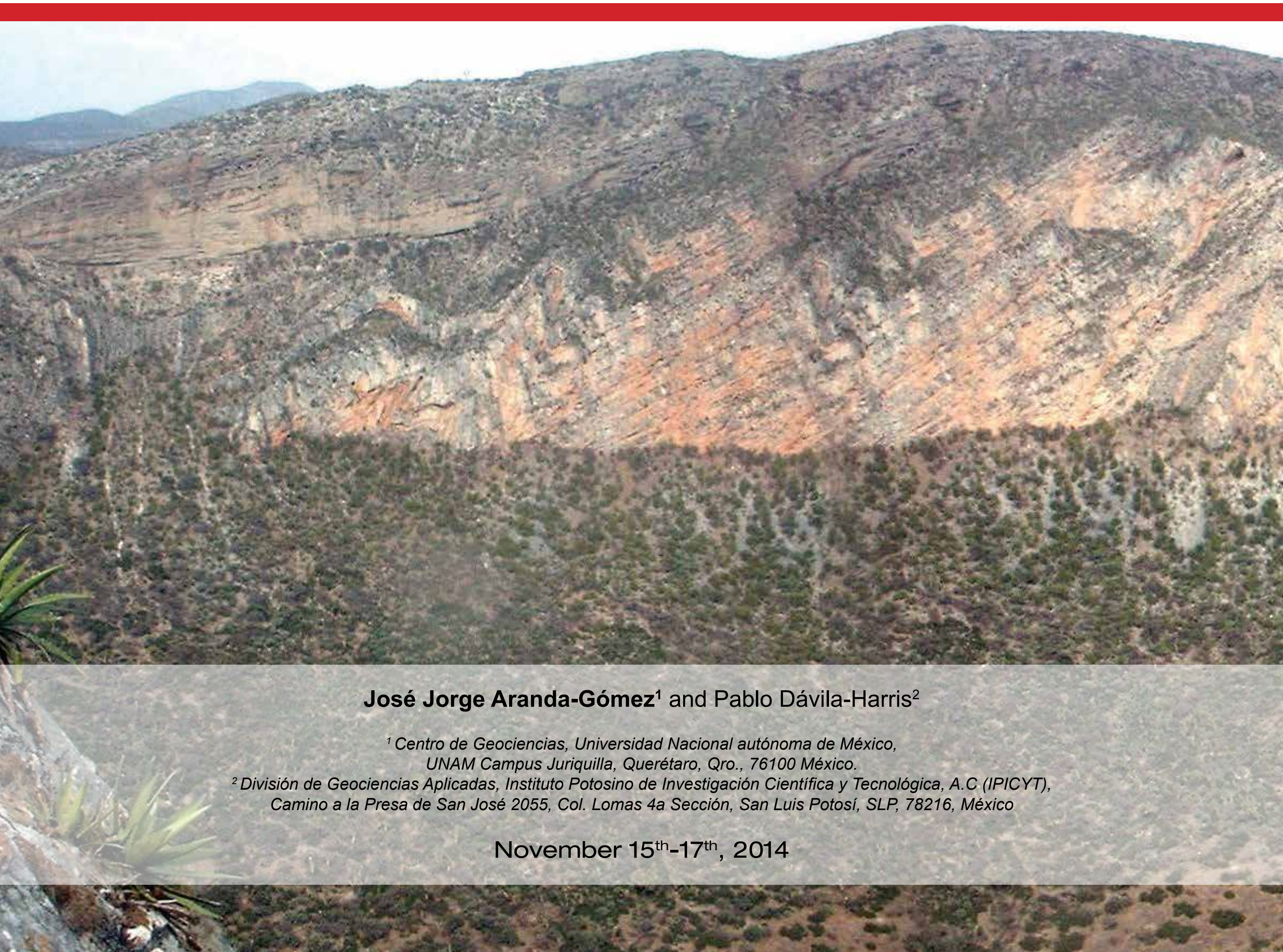

José Jorge Aranda-Gómez[1] and Pablo Dávila-Harris[2]

[1] Centro de Geociencias, Universidad Nacional autónoma de México, UNAM Campus Juriquilla, Querétaro, Qro., 76100 México.
[2] División de Geociencias Aplicadas, Instituto Potosino de Investigación Científica y Tecnológica, A.C (IPICYT), Camino a la Presa de San José 2055, Col. Lomas 4a Sección, San Luis Potosí, SLP, 78216, México

November 15th-17th, 2014

http://maar2014.geociencias.unam.mx

Cover description: Small segment of the Joya Honda crater, San Luis Potosí México.

Universidad Nacional Autónoma de México
Centro de Geociencias

Querétaro, Mexico,
November 2014

Edition and design:
J. Jesús Silva Corona

Maars associated with fracture- and/or conduit-controlled aquifers in folded limestone in San Luis Potosí, México

José Jorge Aranda-Gómez[1,*], Pablo Dávila-Harris[2,**]

[1] Centro de Geociencias, Universidad Nacional autónoma de México, UNAM Campus Juriquilla, Querétaro, Qro., 76100 México.
[2] División de Geociencias Aplicadas, Instituto Potosino de Investigación Científica y Tecnológica, A.C (IPICYT), Camino a la Presa de San José 2055, Col. Lomas 4a Sección, San Luis Potosí, SLP, 78216, México.
** jjag@geociencias.unam.mx, ** pablo.davila@ipicyt.edu.mx*

PART I: OVERVIEW

OBJECTIVES AND SCOPE

This three-day field trip is designed to present the main volcanological characteristics and geologic setting of seven maar-type volcanoes located in San Luis Potosí, central México (Figure 1). Some of these volcanoes are unusual, as they are maars *sensu stricto*, profoundly excavated (up to 200 m) in Mesozoic limestone, and are surrounded by a "tuff cone-like" pyroclastic succession, as Wohletz and Sheridan (1983) use it. The peculiar features of the tephra deposits are: (1) they are well lithified, (2) they are steeply inclined (commonly >15°, and in few places may reach 35°), and (3) a significant portion of the py-

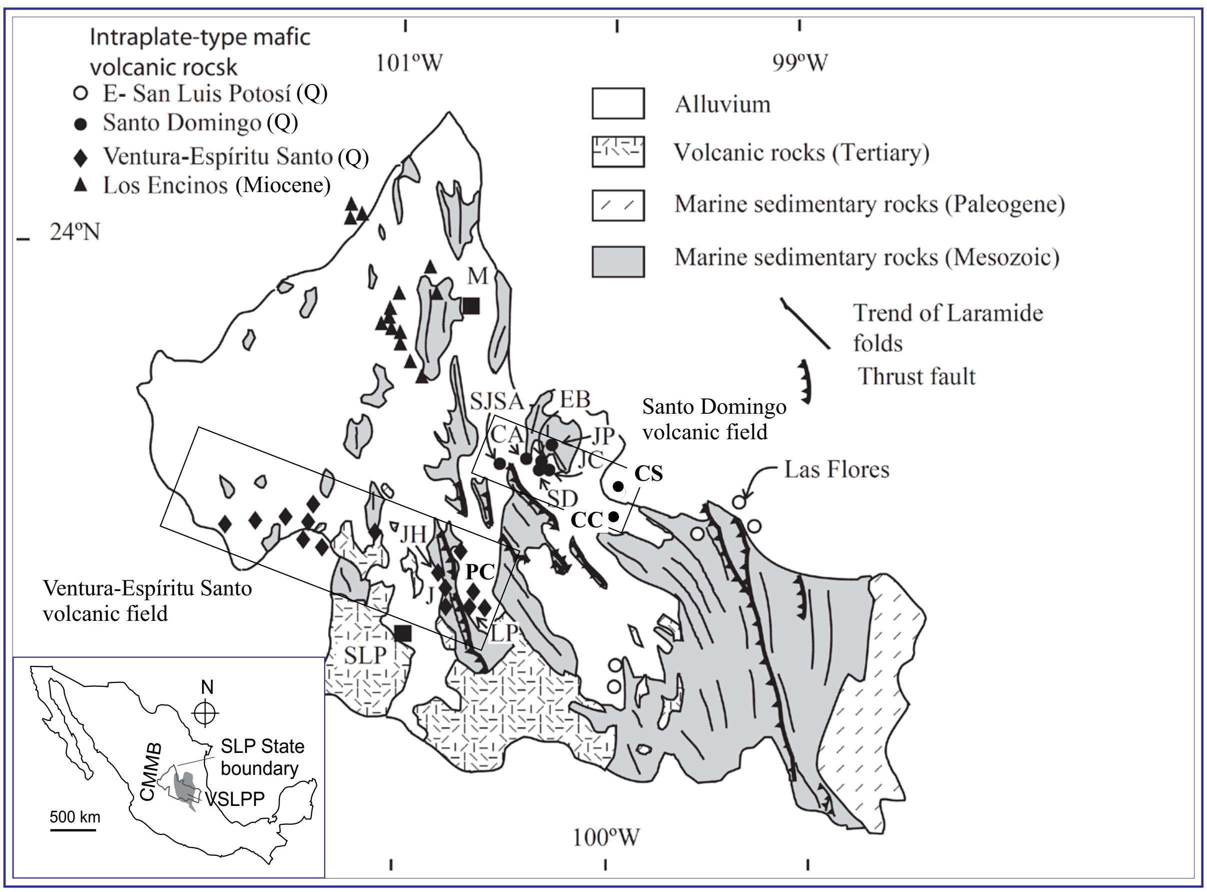

Figure 1. Simplified geologic map of the state of San Luis Potosí showing the location of the intraplate type volcanoes known in it. Key to localities: CA = Cerro El Apaste scoria cone, CC = Cerro Colorado lava field, CS = Cerro Sarnoso lava field, EB = El Banco tuff-ring, JC = Joya de Los Contreras tuff-ring, J = Joyuela tuff-ring, JH = Joya Honda maar, JP = Joya Prieta Maar. LP = Laguna de Los Palau maar, SD= Santo Domingo maar, SJSA = San Juan Sin Agua lava field, and SLP = San Luis Potosí city. (Modified after Aranda-Gómez *et al.*, 2007). Inset shows the location of the Valles – San Luis Potosí carbonate platform (SVSLPP) and the Central México Mesozoic Basin (CMMB), as well as the boundaries of the state.

roclastic succession lacks many of the sedimentary structures that characterize the near-vent deposits around the phreatomagmatic volcanoes elsewhere. We view the Joya Honda maar (Figure 1) as the "type locality" of these structures, as all the extraordinary features listed above are present. The upper 2/3 portion of the near-vent pyroclastic succession in Joya Honda is made of a heterolithologic tuff-breccia, mainly composed by accidental limestone fragments and juvenile nephelinite pyroclasts, with lesser amounts of accidental chert, marl, mantle peridotites and pyroxenites, and lower-crust feldspathic granulites, which range in composition from granitic to gabbroic, and include some paragneisses (Aranda-Gómez, 1982). The tuff-cone like portion of the tephra deposit is: (1) massive to diffusely bedded, and lacks the usual alternation of surge and fall beds produced by repeated hydrovolcanic blasts seen in many maars and tuff-rings tephra deposits, and (2) notoriously lacking in sedimentary features such as low-angle cross-stratification, dunes, antidunes, channels, graded beds, bomb sags produced by ballistic fragments, and load-cast structures caused by fall material deposited atop wet surge deposits.

Some of the San Luis Potosí maar-type volcanoes (Joya Prieta and La Joyuela, Figure 1) are tuff-rings, as their bottom appears to lie above or just slightly below the pre-eruptive surface and exposures of the country rock in the crater walls are very small. The near-vent tephra deposits of these volcanoes display some of the common sedimentary structures found near maars and tuff-rings elsewhere. However, they share with the tephra deposit of Joya Honda the well-lithified nature of their pyroclastic rocks.

All the maar-type volcanoes that we will visit during the field trip were formed during the Quaternary by eruption of mafic, intraplate type magmas and contain mantle and lower-crust xenoliths. The volcanoes have been grouped in two different volcanic fields (Figure 1), based on their association with regional structures, petrology of their lavas, and mantle xenolith assemblages. The Joya Honda and Laguna de los Palau maars, and the Joyuela tuff-ring are located in the Ventura – Espíritu Santo volcanic field. The Joya Prieta and Santo Domingo maars, and El Banco and Joya de los Contreras tuff-rings are part of the Santo Domingo volcanic field. Volcanoes in both fields are low volume features, and appear scattered over relatively large areas, partially covering Mesozoic sediment and/or alluvial deposits.

The Ventura – Espíritu Santo volcanic field is associated with a NW-trending normal fault system, which crosses central México and can be traced for more that 600 km. Some of the rocks in this volcanic field are the most SiO_2 undersaturated Quaternary rocks in the Basin and Range Province so far documented, with less than 42 wt% SiO_2 (all values quoted are normalized, 100% anhydrous, corrected for xenocryst content) and up to 23 wt% **Ne** and less than 4 wt% **Le** in the CIPW norm (Luhr *et al.*, 1989). Spinel-bearing mantle xenoliths in this group of volcanoes usually have coarse-granular texture (Mercier and Nicolas, 1975), and hydrated phases in these mantle peridotites (mostly lherzolites) are absent or extremely rare (Luhr and Aranda-Gómez, 1997).

Most volcanic rocks in the Santo Domingo volcanic field are hawaiites, alkali basalts, with a few basalts with a small amount Hy in the norm., with SiO_2 between 45 and 51 wt % (Luhr *et al.*, 2006). Many of the mantle xenoliths in these volcanoes are foliated tectonites, with well-developed porphyroclastic texture as defined by Mercier and Nicholas (1975). In all the pyroclastic successions associated to these maars, kaersutite megacrysts are very common, in addition to the mantle and lower-crustal xenoliths. Furthermore, there is no doubt that this hydrated amphibole comes from the upper mantle, as composite xenoliths are present. Kaersutite, pargasite, and some phlogopite, together with trace amounts of pyrrhotite and pentlandite, occur as veins and veinlets, cutting the foliation in the mantle tectonites in the composite xenoliths (Dávalos *et al.*, 2011). The Quaternary intraplate volcanoes of the Santo Domingo volcanic field lie on a NW-trending tectonic lineament, which also controls the location of a middle Miocene intraplate volcanic field and of some Oligocene calc-alkaline volcanic centers. There is evidence that the tectonic lineament is a long-lived basement structure that has been reactivated several times, as there are significant changes in the trend of Laramide folds along it.

Joya Honda maar's crater, our type-volcano, is strikingly elliptical in plan view. Its longest axis is orthogonal with the axial plane of Laramide age (late Cretaceous – early Tertiary) anticlinorium ("a composite anticlinal structure of regional extent composed of lesser folds", AGI, 1974) and with a volcanic lineament defined by several intraplate-volcanoes. At the Laguna de Los Palau maar—the only crater excavated in a late Miocene – early Pliocene—an unconsolidated or weakly cemented gravel deposit forms a nearly perfect circle in plan view. All the other maar-type volcanoes in San Luis Potosí have more or less elongated, irregular shapes, whose long axes also tend to be orthogonal to the "tectonic grain" in the nearby Mesozoic limestone. We believe the Joya Honda and Laguna de Los Contreras maars map-view shapes are related to the excavation process caused by the underground phreatomagmatic explosions, which is controlled by the nature of the rocks or sediments involved in the explosions. Thus, these two volcanoes are end members in a continuum, which has at one end hard, anisotropic rocks (Joya Honda) and at the other a soft, nearly isotropic, unconsolidated deposit (Laguna de los Palau, Figure 1).

Finally, during our trip from Querétaro to San Luis Potosí, we will cross a region covered by mid-Tertiary felsic ignimbrites associated to the Sierra Madre Occidental (Figure 2), a large igneous province dominated by felsic ignimbrites (Ferrari *et al.*, 2007). The walls of the Joya Honda and Joya Prieta maars clearly

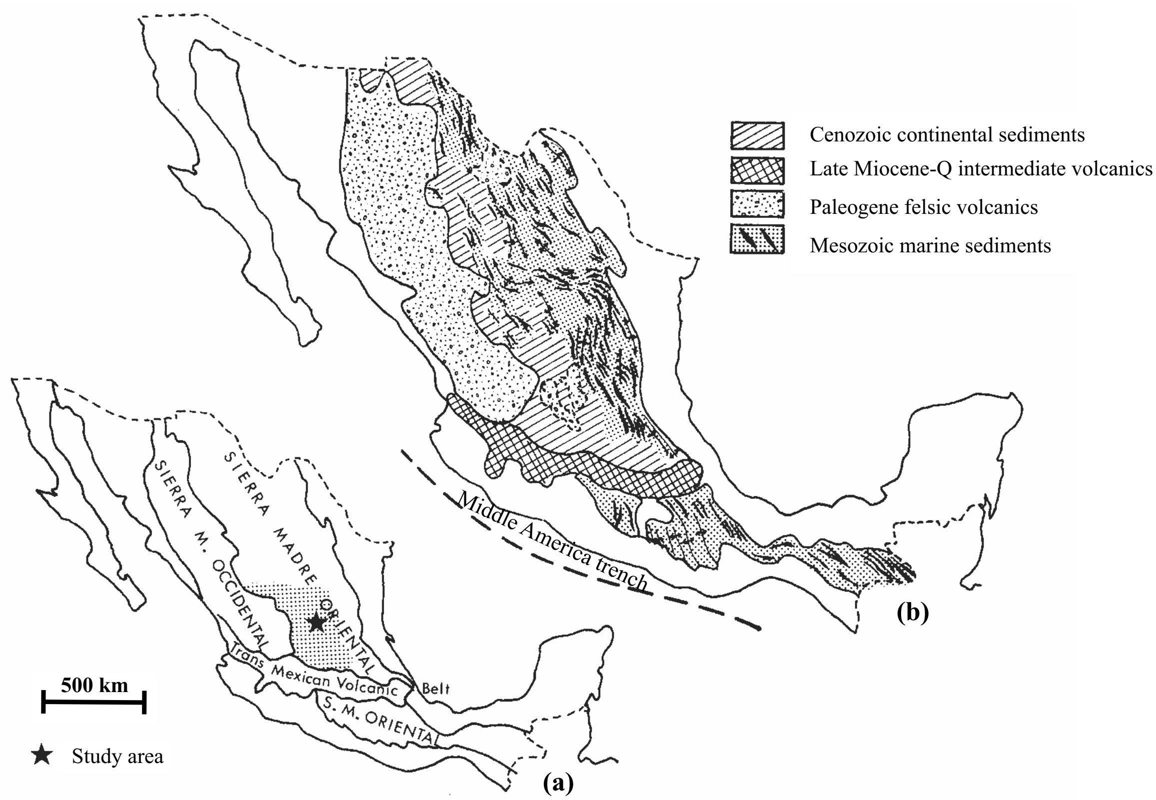

Figure 2. (a) Morphotectonic provinces in central México (simplified after Guzmán and de Cserna, 1963). The stippled area is the region known as the Mesa Central. (b) Geologic sketch map of central México (after Guzmán and de Cserna, *op. cit.*). The different patterns show the age and type of exposed rocks. Curved lines in the Mesozoic sediments show the general trend of the Laramide (late Cretaceous – early Tertiary) structures.

expose deformed sedimentary rocks, characteristic of Sierra Madre Oriental, a part of the North American Cordillera (Figure 2).

As extras to the peculiar geology of the San Luis Potosí maars and their surroundings, we note that they are located (Figure 3) near the southern end of both the Basin and Range province (Henry and Aranda-Gómez, 1992) and the Chihuahan desert (Díaz-Padilla *et al.,* 2011), a fact that creates some peculiar landscapes that our visitors may find attractive. In addition to this, downtown San Luis Potosí, the city where we will spend two nights, has some fine examples of Colonial architecture that the field trip attendants may find worth seeing.

INTRAPLATE MAGMATISM IN CENTRAL AND NORTHERN MÉXICO

Cenozoic (late Oligocene to Quaternary) mafic alkalic rocks occur scattered in the vast region located between the Trans Mexican Volcanic belt and the US–México border (Figure 3a). Many of these intraplate lavas carried xenoliths and/or megacrysts (up to several cm in length) to the surface. The most widespread inclusions found in the intraplate volcanic rocks are mantle peridotites, and/or deep crustal feldspathic granulites, and/or complex sets of megacrysts, which are interpreted as products of the disaggregation of either mantle or crustal xenoliths (*e.g.* Luhr *et al.*, 1995a). Most mantle xenoliths are spinel lherzolite, but spinel-bearing dunite, wehrlite and websterite also occur (Luhr and Aranda-Gómez, 1997). Plagioclase-bearing peridotites are extremely rare and have been identified only at Isla Isabel (Nayarit), which lies on the continental crust at the intersection between the Trans Mexican Volcanic Belt and the Gulf of California (Figure 3a). Among the generally anhydrous feldspathic granulites, those with tonalitic to gabbroic composition are the most common, but there are also granulites derived from pelite, psammite, or granitic rocks. Xenolith-bearing volcanoes usually form low volume and diffuse volcanic fields composed by a few isolated scoria cones and associated lava flows; occasionally in some volcanic fields are a few maar-type volcanoes, together with the scoria cones. Large volcanic fields, whose lava fields cover more than 1,000 km^2 and contain more than 100 vents are exceptional. Most mantle xenolith localities in México are located in the southern portion of the Basin and Range province (Figure 3b) as it was defined by Henry and Aranda-Gómez (1992) or in the Gulf of California extensional province, but xenoliths have also been found in San Quintín (Baja California), which is in the stable portion of the Baja Peninsula (*e.g.* Basu, 1977; Luhr *et al.*, 1995b), and in Llera de Canales (Tamaulipas),

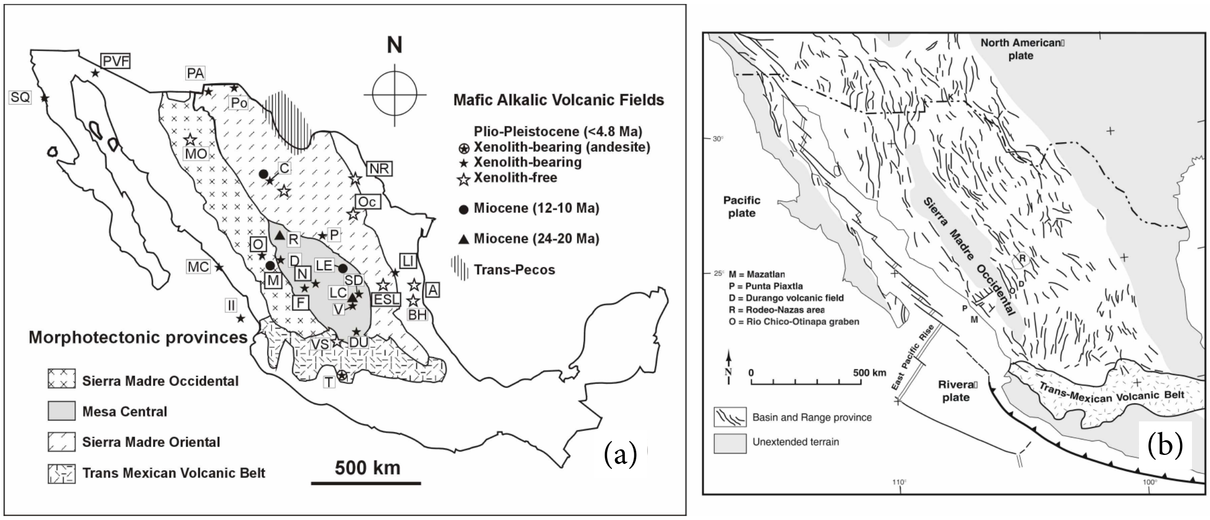

Figure 3. (a) Distribution of intraplate type volcanic fields in central and northern México. Key to localities: A = Aldama, BH= Bernal de Horcasitas, C = Camargo, D = Durango, DU = San Diego de la Unión, ESLP = East San Luis Potosí, F = Fresnillo, II = Isla Isabel, LC = Llanos del Carmen, LE = Los Encinos, Ll = Llera, MC = Mesa Cacaxta, M = Metates, MO = Moctezuma, N = Nieves, NR = Nueva Rosita, Oc = Ocampo, O = Otinapa, P = Parras, PA = Palomas, Po = Potrillo, PVF = Pinacate, R = Nazas ー Rodeo, SD = Santo Domingo, SQ = San Quintín, T = Temascaltepec (with hydrated mantle xenoliths; not an intraplate locality). V = Ventura, V = Valle de Santiago, (b) Generalized map of the Mexican Basin and Range province and location of some of the localities cited in the text.

in the eastern border of the Sierra Madre Oriental (*e.g.* Pettus, 1979; Treviño-Cázares *et al.*, 2005). Both San Quintín and Llera lie outside of the region affected by Basin and Range or Gulf of California extension (Figure 3). Furthermore, there are intraplate rocks that lack deep-seated inclusions, both inside and outside the extended area. These mafic rocks look in the field like “ordinary basalts”, but their geochemistry displays the characteristic enrichment (as compared with subduction related rocks) in TiO_2, Nb, and Ta (Luhr *et al.,* 2006).

The early pulses of intraplate type volcanism were in part contemporaneous with calc-alkaline magmatism and crustal extension in parts of the Sierra Madre Occidental. Mafic alkalic lavas erupted on the Gulf of México’s coastal plain (Figure 3) roughly at the same time as calderas were active elsewhere, closer to the trench. Examples of these alkalic rocks are: the 28 Ma (K-Ar, w.r.) Bernal de Horcasitas volcanic neck (Tamaulipas: Cantagrel and Robin, 1979) and the 24.4-23.9 Ma Nazas-Rodeo volcanoes. (Durango: $^{40}Ar/^{39}Ar$, plag: Aranda-Gómez *et al.*, 2003a). As the volcanic front of the Sierra Madre Occidental arc migrated towards the trench, intraplate magmatism began in areas previously affected by voluminous calc-alkaline volcanism, as shown by the Nazas-Rodeo volcanoes (Figure 3a).

Later, during the middle Miocene, 11.9-11.6 Ma ($^{40}Ar/^{39}Ar$, plag, hbl: Henry and Aranda-Gómez, 2000) intraplate volcanism was simultaneous with a major pulse of extension that originated the proto-Gulf of California and caused the formation of the Río Chico-Otinapa graben near Durango city. The most recent pulse of alkalic volcanism began ~ 4.7 Ma and continued until the late Pleistocene (Aranda-Gómez *et al.,* 2003b). The youngest volcanoes we have successfully dated with $^{40}Ar/^{39}Ar$ are ~ 90 ka and correspond to vents located in the San Quintín and Camargo volcanic fields (Luhr *et al.*, 1995b; Aranda-Gómez *et al.*, 2003b). In several places, such as Isla Isabel, Valle de Santiago, and La Breña – El Jagüey maar complex (Figure 3a), we have obtained “zero” $^{40}Ar/^{39}Ar$ ages. Based on these results and on the undissected aspect of scoria cones, youthful appearance of lava surfaces, and absence of a windblown sand cover, find it reasonable to assume that the youngest intraplate volcanoes might be Holocene in age.

Although most of our understanding on the early pulses of intraplate volcanism comes from a relatively small area near Durango city (Figure 3b), there are a few documented occurrences of this phenomenon elsewhere in southern Texas or in central México. James and Henry (1991) studied 24-17 Ma old mafic alkalic rocks in Trans-Pecos (Figure 3a). We have found at least one locality with a 20.7 Ma (K-Ar, w.r: Tristán *et al.* 2009), intraplate type lavas at Llanos del Carmen in central San Luis Potosí, in the area located between the Ventura – Espíritu Santo and Santo Domingo volcanic fields. Likewise, a large, deeply eroded, 13.6-10.6 Ma volcanic field, made of megacryst-bearing hawaiites occurs in eastern Zacatecas and northwestern San Luis Potosí (Figure 1, Los Encinos volcanic field: Luhr *et al.*, 1995a). Thus, we assume that the early pulses of intraplate volcanism occurred all over central and northern México.

Compared with the number of known early localities, the Plio-Pleistocene volcanoes appear to be considerably more abundant and widespread in the region north of the Trans Mexican Volcanic Belt. However, we are certain that there is a bias in our data, as for a long time we prospected for spinel-lherzolite bearing, "young-looking" volcanic fields. Likewise, we know that extensive volcanic fields as Los Encinos, are now reduced by erosion to a large number of volcanic necks and relatively small lava outcrops scattered on a broad area. Therefore, it is likely that a fair number of deeply eroded volcanic fields of small volume remain to be discovered.

As far as we know, peridotite xenoliths occur only in Plio-Pleistocene mafic alkalic rocks, whereas middle and early Miocene volcanic rocks only carried complex sets of megacrysts and a few, partially digested, xenoliths of feldspathic granulites with mineral paragenesis similar to the accompanying megacryst sets. The geochemistry of the older mafic rocks show clear evidence of ACF processes with crust materials (Luhr *et al.,* 1995a), while younger lavas lack strong evidence of selective assimilation of crustal materials (Pier *et al.,* 1989, 1992). Thus, we believe that rapid magma ascent from the mantle to the surface was favored during the Plio-Pleistocene, as a consequence of a more fractured/extended crust, as compared with the early and middle Miocene. This rapid magma ascent favored the arrival of dense peridotites to the surface and prevented extensive interaction between the magmas with the crust.

EXTENSION IN CENTRAL AND NORTHERN MÉXICO

It is not known precisely when Cenozoic crustal extension began in central and northern México. We have argued that the Guanajuato red bed sequence (~49-36 Ma) probably was formed by accumulation of alluvial fan deposits near the base of block mountains probably bounded by normal faults (Aranda-Gómez and McDowell, 1998). In many localities in central México similar red bed sequences occur between the folded sedimentary marine sequences and the mid-Tertiary calc-alkaline volcanics. Therefore, if our interpretation of the Guanajuato red beds is valid, an Eocene pulse extension may have affected a large portion of central México. We have described thick (>1,000 m) unconsolidated gravel deposits, intruded by a ~ 46 Ma basaltic sill ($^{40}Ar/^{39}Ar$, hbl: Aranda-Gómez *et al.*, 2001) near Camargo (Figure 3a), which is tilted 40-70º and forms a rollover fold, suggesting that accumulation of the deposit and emplacement of the sill were contemporaneous with activity of a nearby normal fault. Faulting and tilting of both gravels and sill occurred prior to the deposition of the Agua de Mayo Volcanic Group (K-Ar, 40-31 Ma, Smith, 1993). Thus, late-middle Eocene extension may have happened as far north as central Chihuahua, near the Camargo Volcanic Field (Figure 3a).

East-northeast extension began in the Oligocene (Henry and Aranda-Gómez, 1992) and it was contemporaneous with Sierra Madre Occidental volcanism. Normal faults have been dated in several places, such as the Pinos mining district (K-Ar, 32-29 Ma: Aranda-Gómez *et al.*, 2007), near the Nazas-Rodeo region (32.3-30.6 Ma: Luhr *et al.*, 2001) and in the Guanajuato mining district (mineralization of Veta Madre, a fault vein, ~29 Ma: Gross, 1975). Younger episodes of normal faulting occurred at the Rodeo half graben at ~24 Ma, the Río Chico-Otinapa graben at ~12 Ma, Juchipila graben (< 5.6 Ma: Carranza *et al.,* 2011), Camargo Volcanic Field (~4.7-2.1 Ma: Aranda-Gómez *et al.*, 2003b), and < 2 Ma in the Durango Volcanic Field (Aranda-Gómez *et al.,* 2003a) and in the San Miguel Allende basin (Carranza-Castañeda *et al.*, 1994).

A GENETIC RELATION BETWEEN EXTENSION AND INTRAPLATE TYPE MAGMATISM?

Most intraplate type volcanoes are located in the region where Cenozoic Basin and Range or Gulf of California extension has occurred (compare Figures 3a and 3b). There are also coincidences in time and space between the volcanic and faulting pulses during the Miocene and Plio-Pleistocene (*e.g.* Aranda-Gómez *et al.*, 2003b), and the idea of several pulses of volcanism and extension comes in part from the study of the intraplate volcanic fields. Thus, it is fair to ask the question: Is extension causing intraplate magmatism or vice versa in central and northern México? The facts that there have been: 1) intraplate type volcanism outside the obviously extended areas north of the Trans Mexican Volcanic Belt (Figure 3), 2) Cenozoic normal faults in a very large number of places where intraplate volcanoes are absent, and 3) intraplate type volcanism (generally without deep-seated xenoliths) occurs in many localities within the Trans Mexican Volcanic Belt (see table 3 in Luhr *et al.*, 2006), outside the Basin and Range and Gulf of California provinces, indicates that there is not such genetic relationship. Luhr *et al.* (2006) stress the point that intraplate magmas within the Trans Mexican Volcanic Belt share many geochemical characteristics with those magmas erupted between the US border and the Trans Mexican Volcanic belt, and these authors reach the conclusion that partial melting of the same type of mantle source generates all the Quaternary intraplate magmas in northern and central México, including the Trans Mexican Volcanic Belt. However, in the case of the intraplate magmas of the Trans Mexican Volcanic Belt there is compelling evidence or mixing with dominant melts generated from a subduction-modified mantle. Mantle and lower crust xenoliths are common in the intraplate magmas of the Northern México Extensional Province, whereas there is only one mantle xenolith locality in the Trans Mexican Volcanic Belt (Temascaltepec: Figure 3b), and a few lower- to middle-crust localities near the limit between the Basin and Range and Trans Mexican Volcanic Belt (Valle de Santiago, the central topic of the intra-conference field trip in the 5IMC) among them. We believe that the protracted extensional history of the region north of the Trans Mexican Volcanic Belt acted as a "ground preparation" and the intense fracturing favored the formation of ascent paths for intraplate magmas. This view is also supported by the fact that some of the most voluminous intraplate volcanic fields, such as Camargo and Durango (Figure 3a) occur at the intersection between major fault systems, such as: 1) the San Marcos fault and the Bolsón de Mapimí in the Camargo Volcanic Field, and 2) the San Luis – Tepehuanes and La Ventana graben in the Durango Volcanic Field, respectively.

REGIONAL GEOLOGICAL SETTING

The San Luis Potosí maars are located in the Mesa Central physiographic province (Figure 2a), in the central part of San Luis Potosí state (Figure 1). The Mesa Central is an elevated region (valley heights range between 1800 and 2100 masl, and the highest points in the mountain ranges may reach 3000 masl), and it is surrounded by three different mountain chains (Figure 2a). To the north and east is the Sierra Madre Oriental, a Laramide age fold and throughst belt, which is part of the North American Cordillera. To the south of the Mesa Central lies the Trans Mexican Volcanic Belt, an active chain of volcanoes, associated with the subduction along the Middle American trench of the Rivera and Cocos plates underneath the North American plate. West of the Mesa Central is the Sierra Madre Occidental, a large ignimbritic province, formed during the Paleogene by volcanic activity related to the subduction of the Farallon plate underneath North America. Both, Sierra Madre Occidental and Sierra Madre Oriental (Figure 2) have been affected by Basin and Range extension during the Neogene and Quaternary (Figure 3).

Outcrop geology in the area where the seven maars are located is dominated by isolated mountain ranges cored by folded Mesozoic marine sedimentary rocks (Figure 1). The most common lithology that we will see during the field trip around the maars is limestone with variable amounts of chert and interlayered marl. In a few places we will see mid-Tertiary volcanic rocks unconformably overlaying the folded limestone or in normal fault contact with them. Broad, flat areas between the isolated limestone ranges are filled by alluvium (Figure 1), as the Mesa Central is an endorheic basin.

Marine limestone facies in the region where the maars are located were controlled by two large paleogeographic features: the Valles – San Luis Potosí calcareous platform (Carrillo-Bravo, 1971) and the Central México Mesozoic Basin (see inset in Figure 1). Mesozoic folding style (Aranda-Gómez *et al.*, 2000), as well as aquifer development and nature (fractured vs conduit-controlled: Aranda-Gómez and Luhr, 1996) were influenced by the calcareous lithologies developed in these two different settings.

The maars were formed during the Quaternary by intraplate-type volcanism, which produced small volumes of pyroclasts and few lava flows that unconformably overlay the limestone or alluvium deposits (Figure 1). Intraplate volcanoes in central and western San Luis Potosí have been grouped into two different volcanic fields, each related to different tectonic features, with significantly different chemical composition, and with contrasting mantle xenolith assemblages (Luhr *et al.*, 1989). The Ventura – Espíritu Santo volcanic field includes four maar type-volcanoes (Joya Honda, Joyuela, Laguna de Los Palau and Pozo del Carmen) and a few tens of scoria cones and associated lava flows, scattered in a broad region, with an area >5000 km^2 (Figure 1). The Santo Domingo volcanic field is about 50 km north of Ventura, across a region where there is no intraplate Quaternary volcanoes, and it is formed by four maar-type volcanoes, <10 scoria cones and associated lava flows, scattered through an area > 1500 km^2 (Figure 1).

Ventura – Espíritu Santo volcanic field

We will see only the easternmost part of the Ventura – Espíritu Santo volcanic field during the field trip, in the area around the small towns of Ventura and Armadillo (Figures 4 and 5). The following description refers mainly to that area.

The eastern portion of this field is located in the limit between the Valles – San Luis Potosí carbonate platform and the Central México Mesozoic Basin. Laramide structures in the region are N20W-trending. As a general rule, the basin carbonates, such as those exposed at the El Coro and San Pedro sierras (Figure 5) usually display tight folds overturned to the NE, while shallow water platform carbonates mostly exhibit symmetric folds with upright axial planes. This portion of the volcanic field is just north of a broad region covered by a thick (up to 1000 m) succession of mid-Tertiary felsic volcanic rocks (Figure 4) of the Sierra Madre Occidental volcanic field, so it is not unusual to see thin remnants of felsic ignimbrites and lava flows lying atop the folded limestone in the area (Figure 5).

The volcanic products of Quaternary maars and cinder cones close to Ventura rest atop Mesozoic marine sediments deposited at the western border of a large carbonate platform. It appears that, for the most part, the transition zone between the platform and the nearby basin, located toward the west, was a gentle slope, where sedimentation was dominated by accumulation of thinly bedded, chert-bearing, carbonate mudstone. In places, this thinly bedded limestone is interlayered with medium to thickly bedded breccia sheets made of clasts derived from the nearby platform. Most volcanoes in the region appear to define a NNW-trending alignment, which is parallel to the trend of the Laramide structures in the region, which are represented by the Sierra de Álvarez and Sierra del Coro anticlinoria (Figure 5). Just at the area where

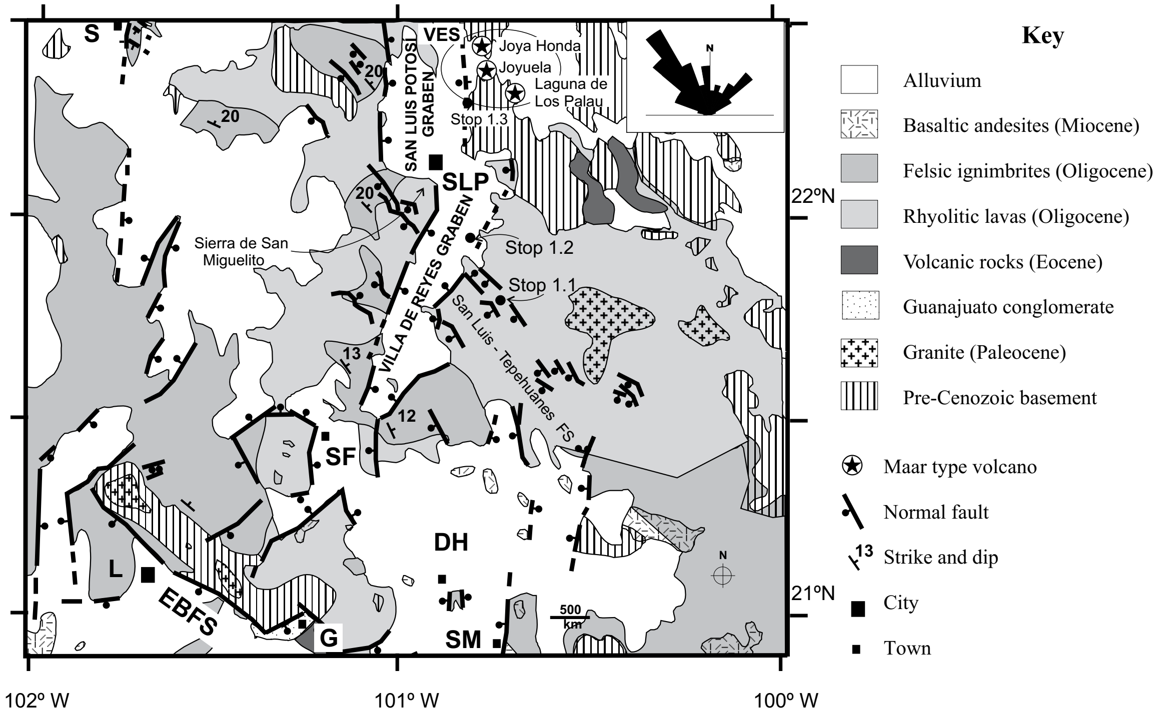

Figure 4. Geologic sketch map of the southern portion of the Mesa Central (modified after Aranda-Gómez and McDowell, 1988) showing the location of the eastern portion of the Ventura – Espíritu Santo volcanic field. The most conspicuous volcanoes in that part of the field are the Joya Honda, Joyuela, and Laguna de los Palau maars. These volcanoes are located about 30 km north of the place where the Villa de Reyes graben intersects the San Luis – Tepehuanes fault system, and close to the San Luis Potosí graben proposed by Tristán González (1986). Inset (a) is a rose diagram of the Cenozoic normal faults in the region taken from Stewart *et al.* (1998). Abbreviations: G = Guanajuato, SLP = San Luis Potosí, S = Salinas de Hidalgo, SF = San Felipe, DH = Dolores Hidalgo, L = León, SM = San Miguel Allende.

Joya Honda and Joyuela are located, there is a small right-lateral displacement of the Laramide structures, and there are at least three volcanic manifestations that define an ENE alignment (see inset b in Figure 5).

The Laguna de los Palau maar was excavated in a gravel deposit accumulated on the eastern slope of the Sierra de Álvarez (Figure 5). The Plio-Quaternary gravel, which we interpret as a "bajada deposit" (bajada: a broad, continuous alluvial slope... extending along and from the base of mountain range, AGI, 1974), rests atop shallow water, thick-bedded, platform limestone. East of the crater are exposed mid-Tertiary felsic volcanic rocks (Figure 5).

The eastern portion of the Ventura – Espiritu Santo volcanic field is 30 km north of the intersection of the NE-trending, 140 km long, Villa de Reyes graben with the San Luis – Tepehuanes fault zone (Figure 4). It is not clear whether the Villa de Reyes graben ends at that intersection or if it changes to a NS trend (or intersects another independent structure) and continues for an additional 150 km to the north (Tristán-González, 1986). We note that in the southern portion of the Mesa Central, in the area depicted in Figure 4, the Cenozoic normal faults have two preferred orientations (see inset a in Figures 4 and 5), that are broadly consistent with the volcanic lineaments defined by the intraplate volcanoes (inset b in Figure 5). Thus, we conclude that intraplate magmas ascended to the surface through extensional structures in the area.

The Santo Domingo volcanic field

These volcanoes are in an area located 50 km northeast of Joya Honda (Figure 1). So far, no Quaternary volcanoes have been found in the intervening area between the Ventura – Espíritu Santo and Santo Domingo volcanic fields. The volcanic field is formed by four maar-type volcanoes, two cinder cones and associated lava flows, and three isolated lava fields, which we interpret as small continental lava shields with high aspect ratios.

The Santo Domingo volcanoes are in an area where there is a pronounced change in the trend of Laramide structures (Figure 6), which we interpret as the product of the influence on Laramide deformation of an older, N50W-trending, basement structure. South of the NW lineament all the Laramide folds trend N45W; north of the lineament they trend NS to N12E. The same NW structure projects to the area south of Sierra de Catorce and crosses the central part of the middle Miocene, intraplate-type Los Encinos volcanic field (Figures 6 and 7). Along this basement structure are located volcanic vents of different ages (Eocene, Oligocene, Miocene, and Quaternary), suggesting that it repeatedly influenced the ascent of magma (Aranda-Gómez and Luhr, 1993). Most mantle xenoliths at the Santo Domingo volcanoes have mylonitic fabrics (Luhr and Aranda-Gómez, 1997), which indicate ductile deformation in the upper mantle, perhaps contem-

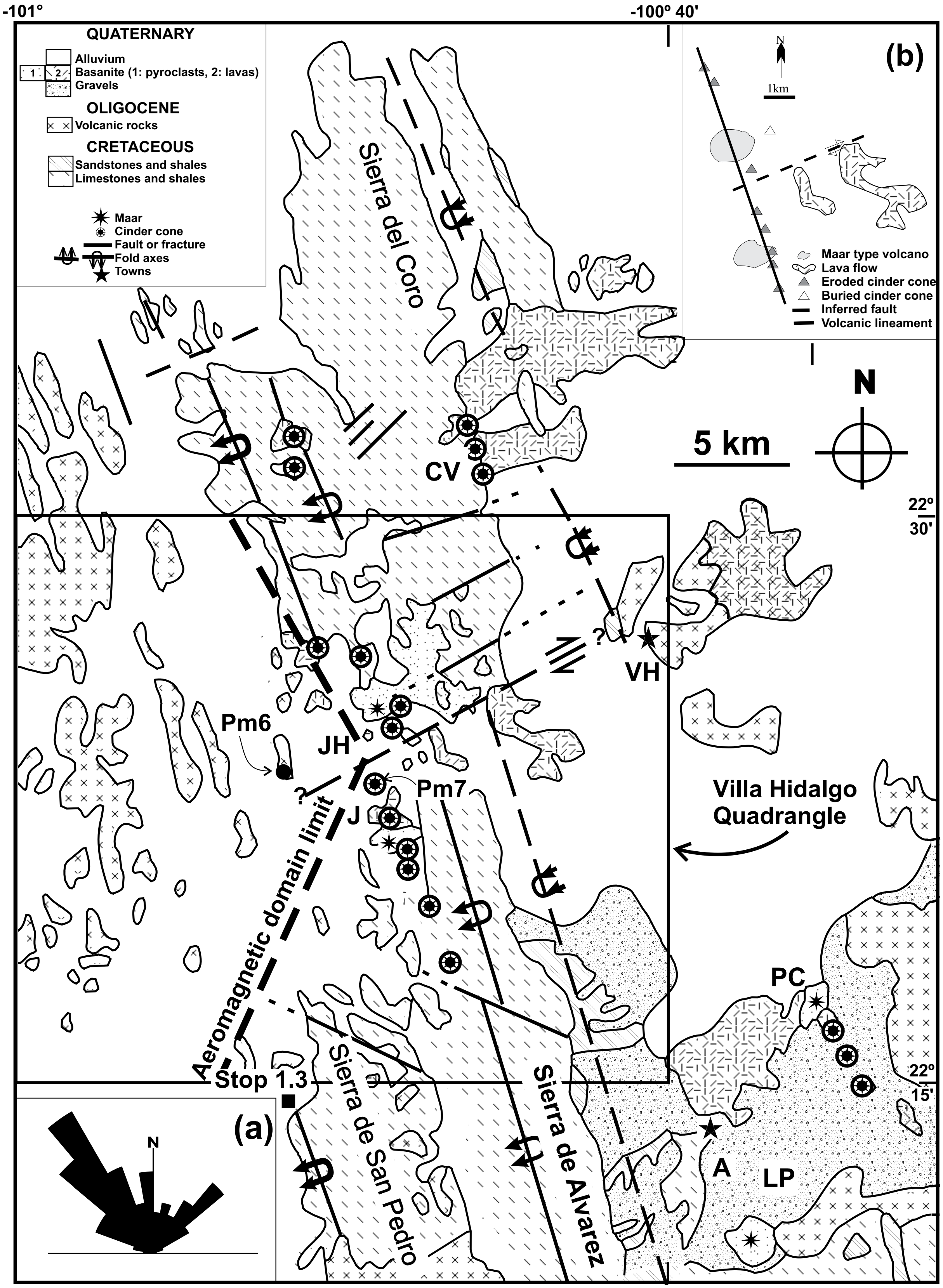

Figure 5. Generalized geologic map of the eastern portion of the Ventura — Espíritu Santo volcanic field (modified after López-Loera *et al.*, 2008). Inset (a) is the rose diagram shown in Figure 4. Inset (b) shows the volcanic lineaments near Joya Honda and Joyuela. Abbreviations: JH = Joya Honda, J = Joyuela, PC = Pozo del Carmen, LP = Laguna de los Palau, VH = Villa Hidalgo, A = Armadillo.

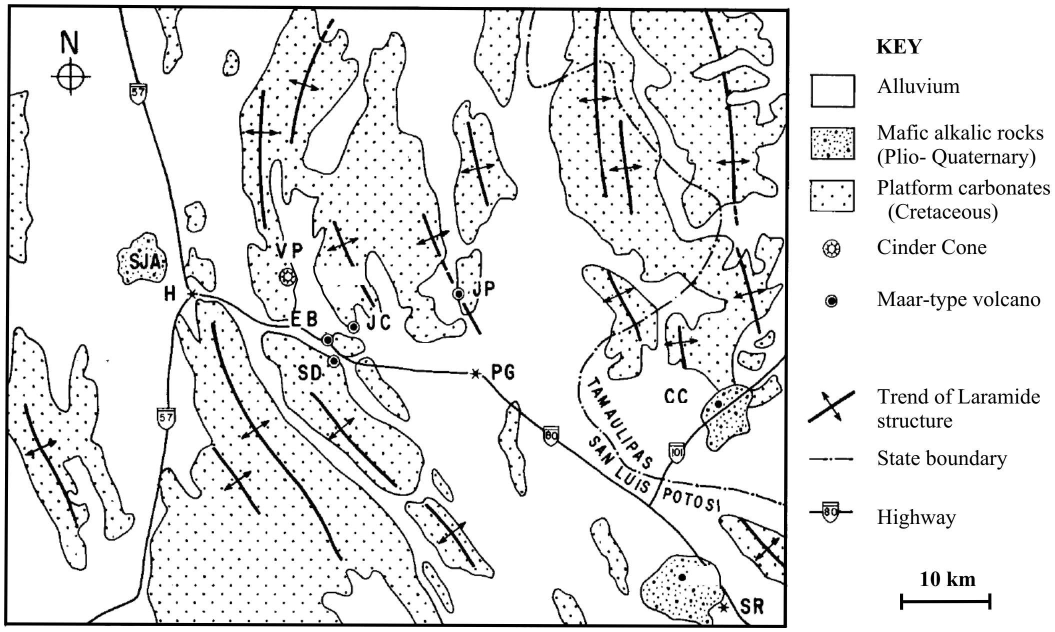

Figure 6. Regional setting of the Santo Domingo volcanic field. Note the pronounced change in the trend of Laramide structures near the area where the Quaternary volcanoes are located. Abbreviations key: SJA = San Juan sin Agua, VP = La Pólvora, EB = El Banco, SD = Santo Domingo, JC = Joya Los Contreras, JP = Joya Prieta, PG = Presa de Guadalupe, CC = Cerro Colorado, SR = San Rafael (Aranda-Gómez *et al.*, 1993)

poraneous with the Quaternary volcanism. Radiometric ages (K-Ar on groundmass separates) obtained for lava samples collected at the Volcán La Polvora scoria cone and Joya de los Contreras are 0.35 and 0.45 Ma, respectively (Aranda-Gómez and Luhr, 1996).

PETROLOGY OF THE PLIO-QUATERNAY VOLCANIC ROCKS OF THE VENTURA – ESPÍRITU SANTO AND SANTO DOMINGO VOLCANIC FIELDS

These rocks were studied in detail by Luhr *et al.* (1989) and Pier *et al.* (1989). General information about intraplate and Quaternary volcanic rocks in México (regardless of their alkalic character) can be found in Aranda-Gómez *et al.* (2007) and in Luhr *et al.* (2006), respectively.

The volcanic rocks from Ventura – Espíritu Santo and Santo Domingo volcanic fields form a well-defined petrological series, which varies from silica undersaturated basanites and olivine nephelinites from Ventura – Espíritu Santo to alkali basalts and hawaiites in Santo Domingo. In both volcanic fields few samples of hypersthene normative basalts associated with the alkalic rocks were found, but they were not studied in detail. The phenocryst and microphenocryst mineralogy of these rocks is Ol + titanaugite (TAug)+ iron-titanium oxides (FTO) $\pm$ Pl. In addition to these primary phases, the rocks commonly include xenocrysts derived from comminution of mantle (Ol + Opx + Cpx + Sp) and, to a lesser extent, from lower crust xenoliths (Q + Pl). Petrographic and chemical distinction between primary and accidental crystals can be made following the criteria described in Luhr *et al.* (1989, 1995a). Pl is always present in the Santo Domingo rocks, but it might be absent in the basanite and nephelinites of the Ventura region.

Silica content in the series decreases in the order: hawaiite (up to 51.2 wt%), alkali basalt, basanite and olivine nephelinite (down to 41.8 wt%). Normative content of nepheline and diopside increases in the same order, while normative content of albite and anorthite are reduced. Many elements – Ti, K, Na, P, Rb, Sr, Zr, Nb, Ba, La, Ce, Nd, Sm, Eu, Hf, Ta, Th, and U have incompatible behavior and increase with normative nepheline. All the Sr and Nd isotopic data plot on or near the mantle array; their distribution is bimodal, although both volcanic fields include samples that fall in both clusters.

Mayor element variations in the suite can be modeled by progressive partial melting of a garnet peridotite in the mantle. In this model, the Santo Domingo magmas represent a higher degree of melting than the Ventura – Espíritu Santo magmas. The Sr and Nd variations can not be explained by a simple partial melting model from a single mantle source, nor can it be explained by crustal contamination. Pier et al (1989) argued that the isotopic variability in the suite requires three different sources in the mantle: 1) a MORB-like source, 2) a Santa Helena-like source, and 3) a hydrated source related to subduction.

Samples from the easternmost portion of the Santo Domingo volcanic field lack xenoliths and have higher $^{87}Sr/^{86}Sr$ without a corresponding decrease in $^{143}Nd/^{144}Nd$. Thus, it is assumed that these magmas, to-

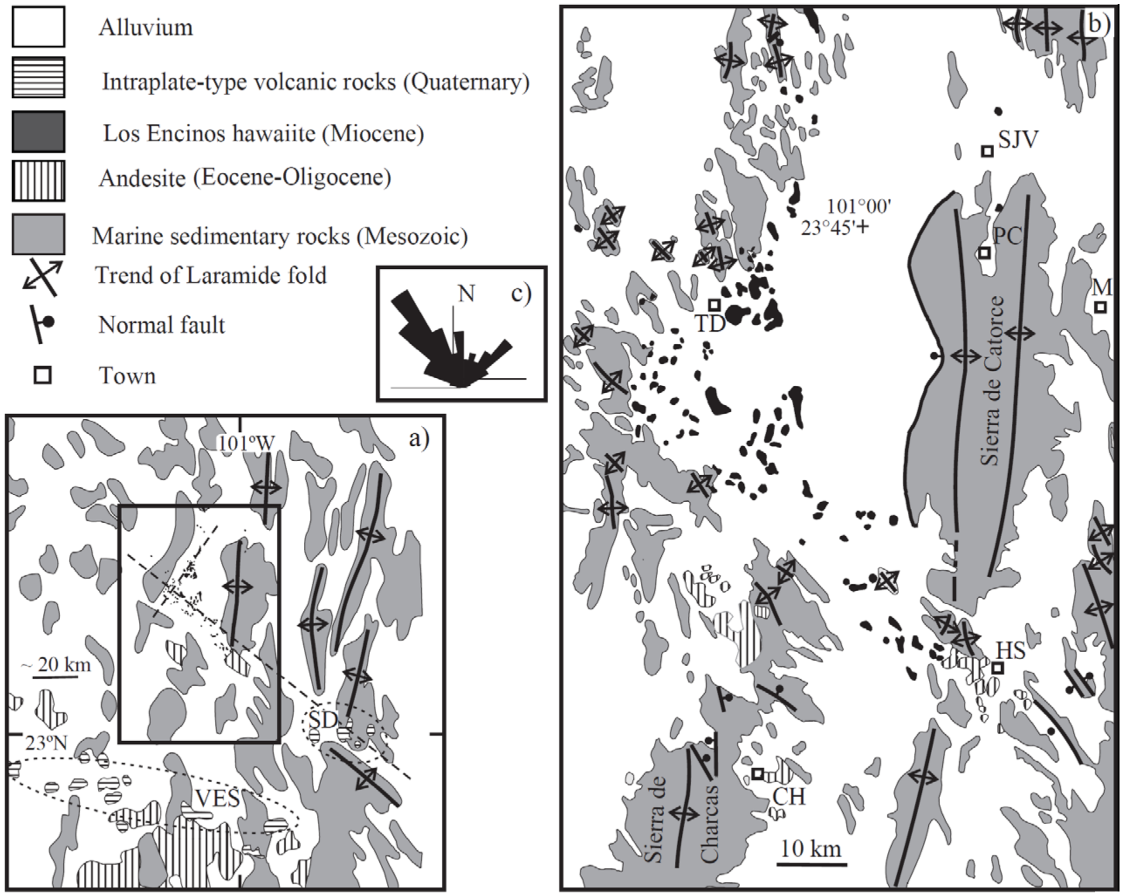

Figure 7. (a) Regional setting of the Miocene Los Encinos (LE) volcanic field and its relation with the Plio-Quaternary Ventura – Espíritu Santo (VES) and Santo Domingo (SD) volcanic fields. Note that Santo Domingo is located along the same inferred basement structure as Los Encinos. The dashed lines correspond to the lineaments mentioned in the text. Key: SJV = San Juan de Vanegas, PC = Potrero de Catorce, M = Matehuala, TD = Tanque de Dolores, HS = Hacienda Solís, CH = Charcas. The box shows the location of the area that is enlarged as Figure 10b. (b) Generalized geologic map of the Miocene Los Encinos volcanic field. Note the change in the trend of Laramide structures along the San Tiburcio lineament and its relation with mid-Tertiary and Miocene volcanic vents in the region. (c) Rose diagram of mid- and late-Tertiary normal faults mapped in the southern part of the Mesa Central. The main trends in the rose diagram correspond with the orientation of the lineaments in Los Encinos volcanic field (Aranda-Gómez *et al.*, 2007)

gether with those in the East San Luis Potosí volcanic field, were contaminated with Sierra Madre Oriental's calcareous rocks, which have high Sr content, high $^{87}Sr/^{86}Sr$ and negligible Nd (Pier *et al.*, 1989).

MANTLE AND LOWER-CRUST XENOLITHS

All the maar-type volcanoes visited in this field trip are important mantle and lower-crust xenolith localities. We know about the existence of more than 20 mantle xenolith localities in San Luis Potosí and about a large number of crustal inclusions in the Miocene Los Encinos volcanic field (Figure 7). The "best" localities, in terms of abundance, size and ease to recovery of the inclusions are the maars.

In order to estimate the relative proportions of the different types of xenoliths in a given volcano a well-exposed outcrop was selected, and in a one square meter area, all the inclusions were identified and counted (Aranda-Gómez, 1982). However, the statistical validity of the results obtained is uncertain, as the study was done in the field with the aid of a hand lens.

A few general conclusions can be drawn from this attempt to establish the relative abundance of xenoliths. Some of these conclusions have been complemented with petrographic study of large xenolith sets collected at each volcano:

1. Spinel lherzolite is the most abundant type in all but two of the Quaternary volcanoes of San Luis Potosí. Hornblendite and kaersutite megacrysts (cleavage fragments derived from large crystals?) are the most common type of inclusion at Joya Prieta (Aranda-Gómez, 1982). Feldspathic granulites are uncommonly large (up to 35 cm) and abundant (90%) at the Cerro del Toro scoria cone in the western portion of the Ventura – Espíritu Santo volcanic field.
2. Kaersutite, hornblendite, and hornblende pyrox-

enite and rare composite xenoliths (foliated spinel lherzolites with hornblende pyroxenite veins) are abundant only in the Santo Domingo maars.
3. Garnet, sillimanite, graphite paragenesis are found in both volcanic fields, but they appear to be more abundant in Cerro del Toro, Laguna de los Palau and Joya Honda
4. Two pyroxene granulites (Pl + Opx + Cpx + FTO ± Q ± Hb) occur in all the localities, but those with garnet and/or spinel are only found in Joya Honda and Laguna de los Palau.
5. All the spinel peridotites have the same mineralogy (Ol + Opx + Cpx + Sp ± Hb), but most xenoliths in Santo Domingo have porphyroclastic texture and the Ventura – Espíritu Santo samples have protogranular texture. Inferred temperatures and pressures of equilibration of the Ventura – Espíritu Santo xenoliths tend to be higher than that of the Santo Domingo samples (Luhr and Aranda-Gómez, 1997).
6. Pyroxenes in the feldspathic granulites from Santo Domingo volcanic field are often partially uralitized and some of the plagioclase is altered to scapolite + calcite. These alterations have been reported for some of the Ventura samples (Ruíz *et al.,* 1983), but they are not as common and intense as in Santo Domingo.
7. Modal metasomatism has only been documented in some of the Santo Domingo peridotite xenoliths. This phenomenon appears to be related to the presence of veinlets of hornblendite in the mantle (Dávalos-Elizondo and Aranda-Gómez, 2011).

ACKNOWLEDGMENTS

Financial support for this research was provided by CONACYT grant 129550 to J. Aranda. Andrés Aranda-López and J. Jesús Silva Corona edited the manuscript; their help is gratefully acknowledged.

§

PART II STOP DESCRIPTIONS

DAY 1
Regional tectonic setting of the Mesa Central and geology of the Joya Honda Maar

Joya Honda is the best studied maar in San Luis Potosí. Several studies on its volcanology, the petrology of its igneous rocks and xenoliths, its geophysics and regional setting, are available. In addition to this, the locality is spectacular and we feel that is the best example of the San Luis Potosí maars. Visiting this locality during the first day of the field trip will give us the opportunity to make comparisons and to point out subtle differences withthe other volcanoes.

Stop 1.1
The N50W-trending San Luis – Tepehuanes fault system, a major structure that influenced intraplate magma ascent in the Ventura – Espíritu Santo volcanic field.

During our trip from Querétaro to San Luis Potosí, we will cross an area covered by mid-Tertiary volcanic volcanic rocks associated to the mid-Tertiary Sierra Madre Occidental volcanic field. These calc-alkalic, felsic, ignimbrites and lava flows are cut by normal faults of the San Luis – Tepehuanes fault system.

Standing at 21° 48' 4.31"N, 100° 42' 57.80"W and looking toward N60W we see a succession of mid-Tertiary ignimbrites. The welded, devitrified portion of the ignimbrites is displaced by NW, down to the SW, normal faults. The faults are slightly younger than the volcanic rocks. This extension episode, broadly contemporaneous with the late phase of volcanism in the region is among the oldest documented in the eastern part of the Sierra Madre Occidental (Aranda-Gómez *et al.,* 2007). These rocks, as most late Cenozoic ignimbrites in the eastern side of the Sierra Madre Occidental are tilted toward the SW (Stewart *et al.*, 1998)

Stop 1.2
An overview of the N45E-trending Villa de Reyes graben. A brief discussion on the Cenozoic extension in the southern part of the Mesa Central. Is the Mesa Central an unusual portion of the Basin and Range province?

We are now leaving the area covered by mid-Tertiary volcanic rocks and descending towards the broad plain where the city of San Luis Potosí is located.

Standing at 21° 58' 42.64"N, 100° 48' 46.97"W and looking toward S26W we see a broad tectonic valley, which can be traced for 120 km to the SW. In its southern end, the graben ends at the N50W-trending El Bajío normal fault system (Figure 4), which is the tectonic boundary between the Mesa Central and the Trans Mexican Volcanic Belt. El Bajío fault has had vertical displacement close to 800 m in the last 10 Ma (Aranda-Gómez *et al.*, 2012)

In its north end, close to the place where we are standing, the graben intersects the N55W-trending San Luis – Tepehuanes fault system, which is essentially parallel to El Bajío fault. It is not clear if the Villa de Reyes graben ends here or if it is displaced, or if it changes direction. Figure 4 shows Tristán-González interpretation; he believes that the structure changes direction and becomes the San Luis Potosí graben. The age of the graben is also broadly contemporaneous with the Sierra Madre Occidental volcanism as it has been argued that the distribution of some volcanic units was controlled by this tectonic depression (Labarthe-Hernández *et al.*, 1982).

N25E of us is the Sierra de San Pedro, which is formed by folded limestone. Most sediments of the Sierra de San Pedro were deposited in the Central México Mesozoic Basin, close to the Valles – San Luis Potosí calcareous platform. Capping the Mesozoic marine sediments are remnants of the mid-Tertiary volcanic rocks. North of us is the area where Joya Honda and Joyuela are located.

Stop 1.3
A panoramic view of the western flank of the Sierra de San Pedro. Is this mountain range flanked by NNW-trending Cenozoic normal faults, which are essentially parallel to the trend of Laramide structures?

In many localities of central and northern México, the general trend of Laramide folds and Basin and Range faults is parallel. More than 40 years ago, De Cserna (1969) pointed out that in the Chihuahuan desert, near the México – USA border it is difficult to establish whether the "Basin and Range morphology" of that area was formed by extension or if the morphology reflects a succession of alluvial valleys occupying synclines alternating with elongated mountain ranges corresponding to anticlines. The same problem appears to be present in this portion of the Mesa Central.

Here (22° 14' 50.81"N, 100° 49' 32.75"W), looking in a S70E direction we can see the Cerro El Pintonte, a locality where a flat-laying remnant of the mid-Tertiary volcanic rests atop the folded limestone.

The same volcanic unit is exposed at the base of the range, directly N of where we stand. Height difference between these outcrops is in the order of 350-400 m. Thus, it is fair to assume that the SE flank of Sierra de San Pedro might be controlled by a N25W-trending normal fault, which is parallel to the trend of the Laramide structures. It is worth pointing out that most intraplate volcanoes in the eastern part of the Ventura – Espíritu Santo lie along this same trend (Figure 5). Suter (1991) used part of this Ventura volcanic lineament as evidence to infer the stress orientation at the time of volcanism (Plio-Quaternary).

Stop 1.4
A first look to the Joya Honda's crater. Form and general dimensions of the maar. A panorama of the southern wall of the crater.

We are standing on Joya Honda's near-vent pyroclastic succession, near the edge of the crater (22° 25' 21.06"N, 100° 47' 0.32"W). This vantage point gives an excellent view of the southern wall of the crater where folded limestone is exposed.

Joya Honda is a maar *sensu stricto,* as it clearly exposes pre-volcanic rocks on its walls. The maar is a large, ellipitical crater, with axes 1100 and 850 m long (Figure 8) oriented N67E and N23W, respectively. Maximum relief from the floor of the crater to the highest point in the tephra deposit is approximately 300 m and it occurs 750 m west of the place where we are standing. The height of the crater on its southern wall is 240 m, as in that area (S20W of Stop 1.4) the near vent succession was not deposited. The floor of the maar is nearly flat, with major and minor axes 400 and 250 m, respectively. Near the base of the nearly vertical walls of the crater there is a steep talus deposit, which is partly masked by vegetation.

North of the place where we parked the vehicles is Sierra El Coro, which is formed by folded limestone accumulated in the Central México Mesozoic Basin. Just at the base of Joya Honda's pyroclastic rampart, there is a broad, flat agricultural area with a general elliptical shape that resembles some of the tuff rings in the area. On the western side of that area (N55W from where we are standing) there is a near-vent pyroclastic deposit, of uncertain affiliation. It could be part of Joya Honda or it could belong to another maar-type volcano. A magnetic survey performed by López-Loera *et al.* (2008) showed the existence of negative anomaly centered in that area. However, this feature is interpreted as part of the bipolar anomaly produced by Joya Honda (Figure 9).

Stop 1.5
The base of Joya Honda's tephra deposit as seen on the eastern part of the crater. A pre-maar scoria fall deposit covered by a paleosol and spring (or caliche?) deposit. The nature of the first pyroclastic bed associated to Joya

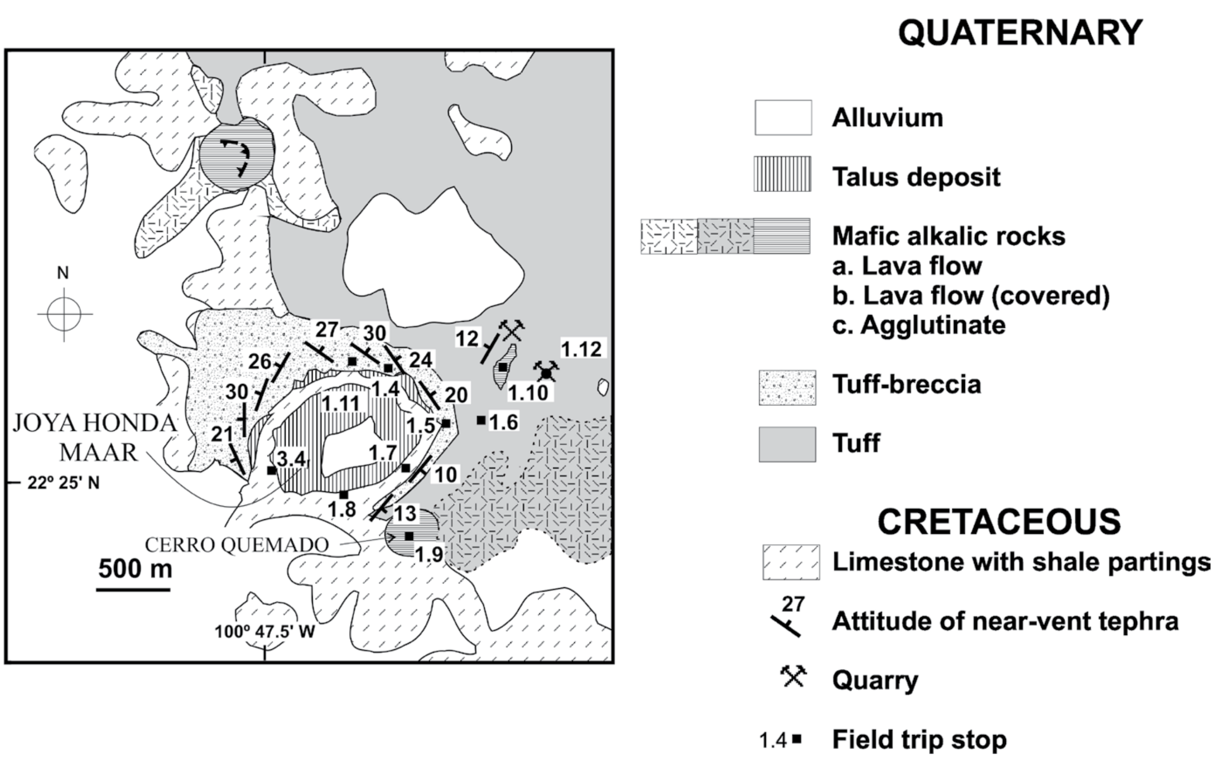

Figure 8. Geologic map of Joya Honda (modified after Aranda-Gómez and Luhr, 1997 and López-Loera *et al.*,, 2008).

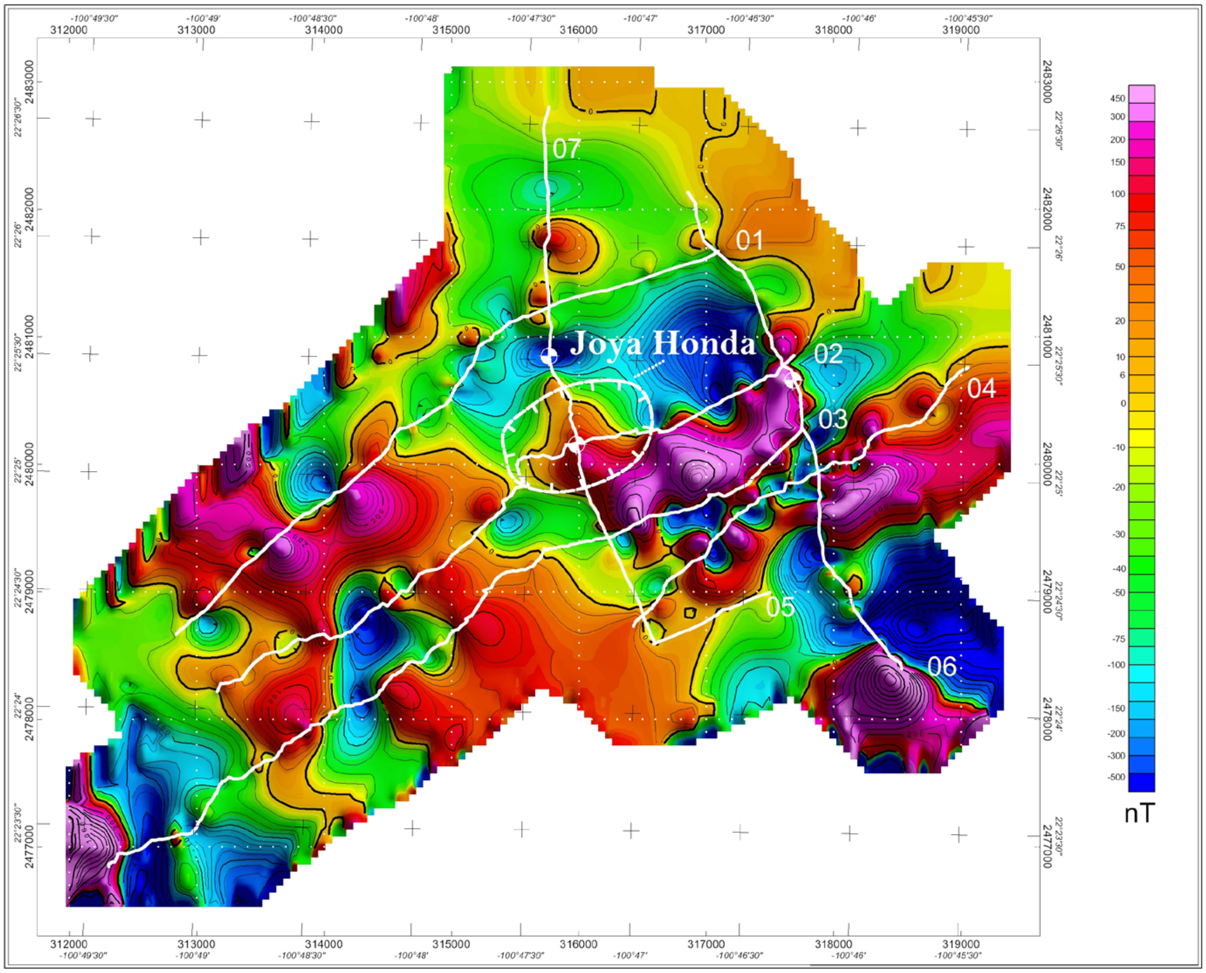

Figure 9. Configuration of the residual magnetic field based on data collected in ground surveys around Joya Honda (white ellipse). Note the bipolar magnetic anomaly associated with Joya Honda. White lines show the location of magnetic profiles 01-07. White circles are the sites where electrical vertical soundings and audio-magnetotelluric soundings were performed. Doted black lines within the crater are the gravity profiles (from López-Loera *et al.*, 2008)

Honda's eruption. Beginning of a traverse where we show the stratigraphic section measured by Aranda-Gómez and Luhr (1997).

From Stop 1.4, we will walk on a trail heading toward the east. In few places the trail is steep so we recommend caution to avoid a fall. In this area there are abundant chollas (a very aggressive cactus with spines that may puncture leather boots and that some times "jumps" and adheres to the legs or even higher in the body). We recommend avoiding these cactus in order to prevent an unpleasant and painful experience. As we get close to the site where the stratigraphic log begins (Figure 10) we can see a panoramic view of the pyroclastic succession, where three near vent stratigraphic units can be easily distinguished.

At 22° 25' 10.45"N, 100° 46' 52.97"W are exposed intervals 1 to 9 (Figure 11). Intervals 1 to 3 are located below the trail in a very narrow space. Intervals 4 to 9 are at or above the ground level at the trail. Again, we recommend extreme caution to those willing to take a close look into intervals 1 to 3 as the outcrop is very close to the vertical wall of the crater.

It is worth stressing that Joya Honda's very first pyroclastic bed, about 3 cm thick, which lies above a paleosol, is an open framework, fine grained, well rounded, and sorted heterolithologic deposit. The rock completely lacks matrix and is made of rounded clasts of dense olivine nephelinite, limestone, chert and xenocrysts from the deep-seated xenoliths. The clasts are bound together by a calcite and/or zeolite (?), crustified cement.

As the pyroclastic succession is exposed on a nearly vertical wall, Aranda-Gómez and Luhr (1997) described the log along the trail, but before we leave this site, we encourage the participants to pay attention to the overall structural attitude of the limestone beds and their relation with the slope of the crater's wall; they both are essentially vertical and parallel.

The fine grained tuff at the base of the succession is interpreted as a relatively "dry" surge deposit, and dis-

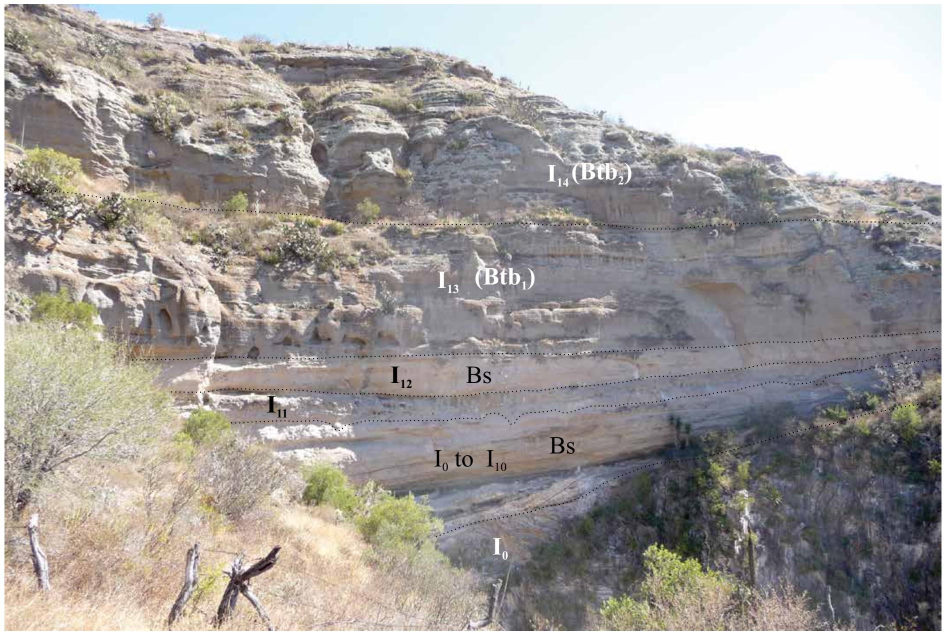

Figure 10. Panoramic view of the section described by Aranda-Gómez and Luhr (1997). Some of the intervals shown in Figure 11 are labeled in the photograph.

plays sedimentary structures such as small channels, low angle cross bedding, accretionary lapilli beds, fine lamination, and internal graded bedding, among others. These tuffs are fine-grained and sedimentary and juvenile clasts "float" in matrix made of finely comminuted limestone, which appears as a cryptocristalline aggregate under the microscope. In general, juvenile clasts are non-vesiculated and unaltered (not hydrated). Remarkable features of this early, 7 m thick, base surge deposit are that it tends to be well cemented and it lacks the interlayered fall deposits seen in other near-vent phreatomagmatic deposits. It is only at the base of interval 11, a very poorly sorted, fine to medium gravel (1-2 cm) with 15 % large (up to 55 cm) angular blocks of limestone, where conspicuous bomb sags can be seen. We interpret interval 11 as a fall deposit, which is in turn covered by another, 1.5 m thick, base-surge deposit (interval 12) similar to intervals 4 to 10 (Figure 10).

When we arrive to 22° 25' 8.94"N, 100° 46' 53.54"W we will leave the trail and turn east toward Stop 1.6.

We are now at Btb1 and the rest of the stratigraphic section is made of tuff-breccia, the unit that makes the bulk of the near vent deposit of Joya Honda. As we move upsection we will see that the juvenile clasts become progressively more vesiculated and palagonitized. Also common in this rock, are rounded, slightly vesiculated palagonite fragments with internal jigsaw cracks, characteristic of vitric hydroclastic shards (Fisher and Waters, 1970). The glass is bright orange to red.

Stop 1.6
End of the traverse and interpretation of the stratigraphic section. Evidence of a sudden water increase in the eruptive system and depressurization of the vent

We are now near the top of the pyroclastic succession, at interval 14 (Figure 11).

Here, 22°25'8.76"N, 100°46'51.58"W, some the juvenile clasts are "frothy" palagonite and coexist with moderately vesiculated clasts of palagonite and rare fragments of non-vesiculated nephelinitic glass.

Aranda-Gómez and Luhr (1997) interpreted this pyroclastic succession as follows: "at the onset of the eruption, magma began to interact with moderate amount of groundwater, producing the dry-surge deposits [intervals 4-10 and 12]...As the eruption continued, the crater grew and the hydrovolcanic blasts fractured the limestone around the explosion foci. A marked increase in the water/magma ratio of the system followed when a large fracture or a portion of the limestone with enhanced secondary permeability was intersected by the expanding crater. Subsequent phreatomagmatic explosions occurred in a system with groundwater flow rates several orders of magnitude larger than the initial dry-surge stage....Juvenile clasts in the near-vent deposits show a marked upward increase in both hydration (palagonitization) and vesicularity. The increase in palagonitization … appears to be a consequence of the overall increased wetness of the eruption with time... The transition toward higher vesicularity is interpreted

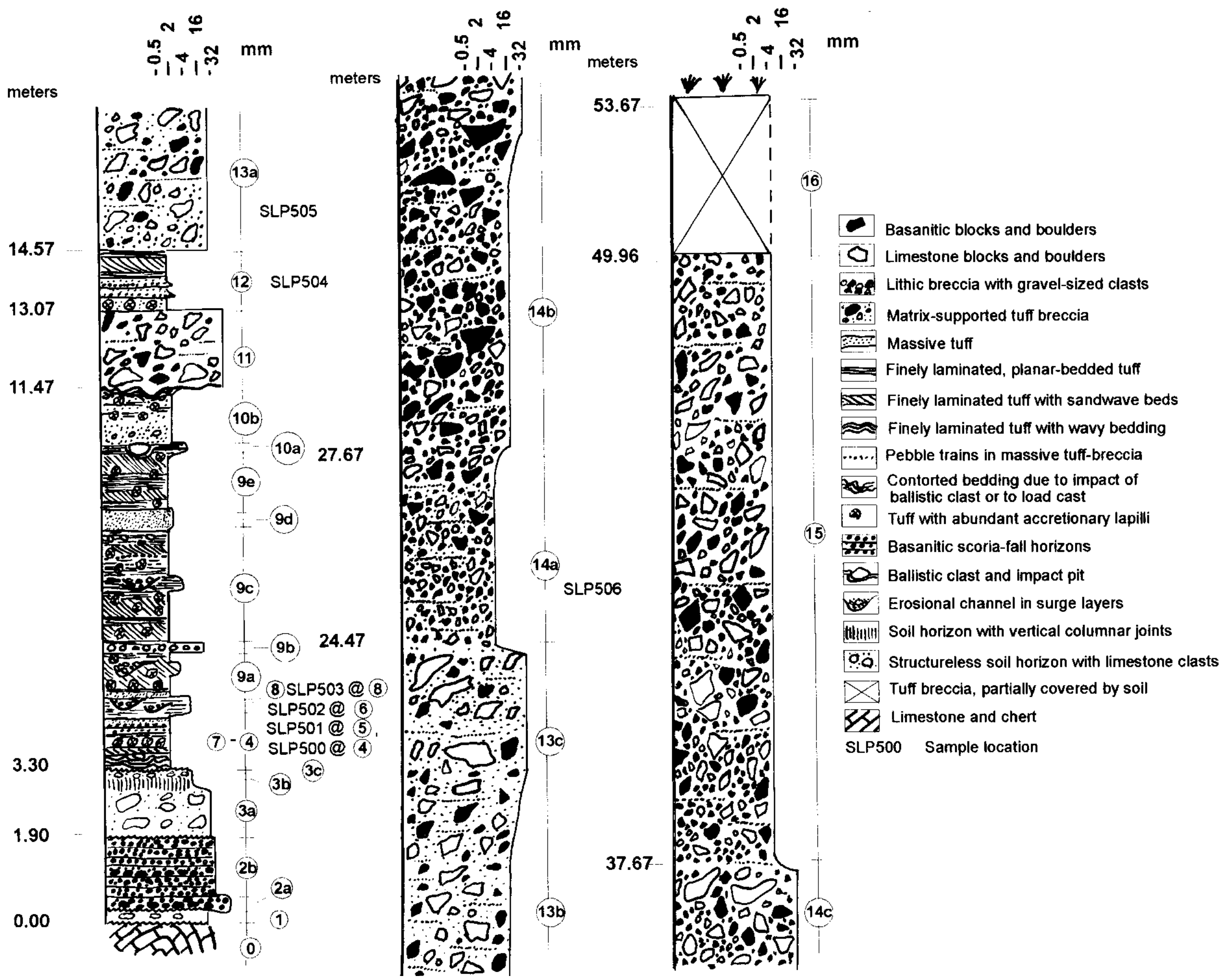

Figure 11. Stratigraphic section measured in the eastern wall of Joya Honda, between Stops 1.5 and 1.6 (Aranda-Gómez and Luhr, 1997). White accidental clasts in the near vent tuff-breccia are mostly limestone and chert, with a small amount of propylititized andesite (mid-Tertiary?) and deep-seated xenoliths (mantle peridotites and feldspathic granulites). Grain size scales at the top of each column show visual estimates of the median clast sizes. The three near-vent units that can be distinguished in the vertical walls of the crater are: 1) Base-surge tuff (intervals 4 to 12), 2) Basaltic tuff-breccia one (Btb_1: interval 13), and 3) Basaltic tuff-breccia two (Btb_2: intervals 14 and 15). Distinction between the two tuff-breccias is based in overall color of the deposit, which depends on the limestone-nephelinite clast proportion in the rock and bedding in the deposit. Btb_1 is a tan-colored, heterolithologic, massive to diffusely bedded, heterolithologic tuff-breccia, while Btb_2 is a distinctly bedded, medium brown, heterolithologic tuff-breccia.

as evidence of a gradual reduction in the confining pressure for the ascending magma prior to explosive fragmentation....”

Stop 1.7
A small outcrop of scoria-fall (or surge?) near the base of the pyroclastic deposit of Joya Honda. Was there an initial strombolian phase at the beginning of Joya Honda’s eruption?.

From Stop 1.6 we will go back to the trail and follow it toward the southeastern part of the crater.

This is an outcrop that was not taken into account by Aranda-Gómez and Luhr (1997) model about the origin of Joya Honda. We note that this occurrence does not invalidate the general model of Aranda-Gómez and Luhr (1997) as it implies that external water did not have access to the vent early in the eruptive history of the maar. We also stress that there is no way of correlating this particular deposit with the scoria-fall deposits seen in Stop 1.5, as those beds clearly are covered by a paleosol, which implies a significant time interval between their deposition and the beginning of Joya Honda’s eruption.

Furthermore, the following features observed at this site: the scoria-rich deposit was accumulated in an erosional channel flanked by surge deposits. Likewise, we also notice that the scoria deposit grades upward to a base surge deposit, with a smaller proportion of juveniles. Thus, it might be that this facies is also phreatomagmatic in origin and the main difference with other facies observed near the edge of the crater is that it contains an unusually high proportion of nephelinite clasts.

Stop 1.8

A panoramic view of Joya Honda's northern wall. The pre-maar paleosurface. Absence of tephra deposits on the southern wall of the crater. Thickness variations of the tephra deposit around the maar and evidence of directed blasting. General discussion about the Laramide structure and the role of medium- to thick-bedded breccia sheets interlayered with basin carbonates. What was the nature of Joya Honda's aquifer; fracture or conduit dominated?

From this vantage point (22° 24' 51.79"N, 100° 47' 8.71" W) we see an impressive panorama (Figure 12) of the northern wall of Joya Honda. There are several features that are worth mentioning:

1. The pre-maar surface it is clearly seen between the folded limestone and the pyroclastic sequence. There is a conspicuous angular unconformity between these units. The shape of the pre-maar surface implies that at the time of the eruption there was no clastic deposit where a darcian aquifer could be hosted. Therefore, water came from a fracture- or conduit-controlled aquifer in the Mesozoic rocks. We believe that limestone in Joya Honda's area was accumulated in the Mesozoic basin and contains significant amounts of clay and chert that prevent the formation of karstic features. However, interlayered with the medium to thinly bedded basin carbonate, are thicker breccia sheets made of materials derived from the nearby platform. These cleaner carbonates may have selectively developed dissolution conduits.
2. The maar was excavated near the core of an anticlinorium. We note that the overall shape of the Laramide structure is an arch, but is composed by lesser folds. Likewise, we point out that most limestone layers are inclined toward the SW as the NE flank of the structure is overturned.
3. There are marked changes in the bed thickness in the limestone. In places it is thinly bedded and tightly folded, and other layers are considerably thicker and less deformed. Thus, it seems that deformation style was controlled by the mechanical properties of the thin and thick beds.
4. The general attitude of the layers in the pyroclastic deposit mimics the shape of the pre-maar surface.
5. The thickest pyroclastic section occurs on NNW part of the crater. The pyroclastic rampart thins toward the SW and SE, and finally disappears in the southern wall (the place where we are standing).
6. The overall distribution of the distal, ash-fall deposits of Joya Honda (Figure 8) is toward the NE. These ash-fall tuffs reach a distance of 6 km from the center of the crater. However, near-vent facies can be found only 850 m away of the center of the crater in the NE direction, while they can be found up to 1.5 km away from the center. Therefore, we conclude that Joya Honda's blasts were directed toward the NNW while the wind was blowing to the NE.
7. Secondary permeability in the limestone is at least in part related to tensional fractures sub-parallel to the axial plane of the anticlinorium.

Stop 1.9

The Cerro Quemado remnant and the hypothesis behind the magnetic survey around Joya Honda.

We will walk 400 m downhill toward the S57E to the Cerro Quemado. Hopefully, we will find some evidence about the relative age of this vent respect to Joya Honda. Luhr et al (1989) reported a sample collected here as a post-maar lava. Later, López-Loera et al. (2008) re-interpreted this outcrop as a deeply eroded, pre-maar scoria cone (?). One of the problems associated with this outcrop is that Joya Honda's pyroclastic succession rapidly pinches out in

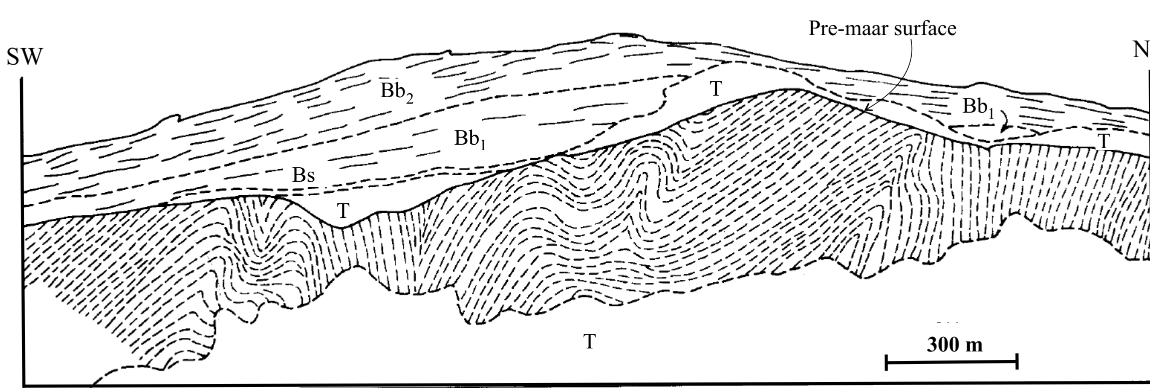

Figure 12. Geologic sketch of the northern wall of Joya Honda's crater. The near vent pyroclastic succession rests directly atop the folded marine carbonates. The pre-maar surface can be clearly seen and it is obvious the presence of buried hills and fluvial valleys. The sketch also shows the influence of the buried pre-maar surface in the structural attitude of the overlaying pyroclastic succession. Units depicted: T = Talus deposit, Bs = base surge tuff, Bb1 and Bb2 = the near-vent upper and lower tuff-breccias. Note the complex Laramide folding in the Mesozoic limestone (Aranda-Gómez, 1982).

the area so it is not easy to find the contact relation between the scoria or lava (?) with Joya Honda's tephra.

In Stop 1.4 we mentioned a magnetic survey performed by López-Loera et al (2008) and Figure 9 is one of the illustrations of that paper. This locality is a convenient place to expand the information about this study.

We are standing (22° 24' 44.97" N, 100° 46' 57.02" W) on top of an outcrop of olivine nephelinite. Based on the results of their magnetic survey and in the nature of the exposed rocks, López-Loera *et al.* (2008) concluded that this is an erosional remnant of a relatively old scoria cone. Seen in the aerial photographs this volcano presents no vestiges of a crater. The aeromagnetic study and ground magnetic survey had, among others, the following goals: (1) Investigate if there is a diatreme under the Joya Honda crater as implied by Lorenz (1986) model, and 2) Find out if there is a feeding dike (*e.g.* Figure 2 in Lorenz and Kurszlaukis, 2006) connecting the intraplate volcanoes in the Joyuela – Joya Honda volcanic lineament (Figure 5, inset b). The idea behind this geophysical survey was based on the fact that there is a large contrast in magnetic susceptibility between the olivine nephelinite and basanites of the Ventura – Espíritu Santo volcanic field and the carbonate-dominated country rock. Thus, if a diatreme exists underneath the crater and a dike joins the volcanoes, both features could be detected. Figure 13 shows the magnetic profiles 03 and 05 (see their location in Figure 9). From this point we can see the hills where profile 05 was measured, and the area where profile 03 started.

Stop 1.10
Near-vent agglutinate related to a pre-maar vent. Origin of the scoria-fall deposit exposed at the quarry located NE of the maar. Isotopic age of Joya Honda.

There is nothing remarkable about this outcrop. Here at the top the hill is a small exposure of agglutinated scoria, which is interpreted as a near-vent deposit. Aranda-Gómez and Luhr (1997) dated it (K-Ar, matrix separate) at 1.1 ± 0.21 Ma and interpreted it as post-maar material. If this is true, Joya Honda must be older than 1.1 Ma.

There are two large quarries on the NE and NNW sides of the hill where we are standing. The material mined at the quarries is a relatively well sorted, distinctly bedded, scoria-fall deposit. Most fragments are nephelinitic scoria, but there a few isolated clasts of limestone and chert in this unit.

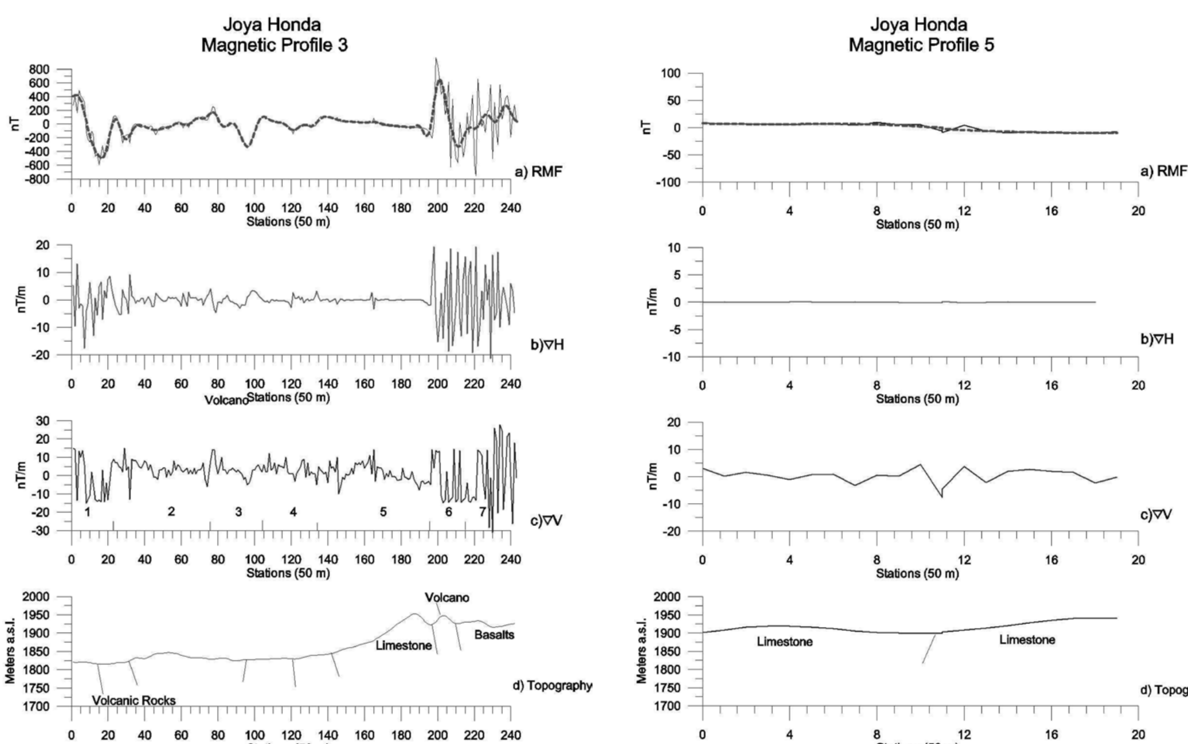

Figure 13. Magnetic profiles 03 and 05 (López-Loera *et al.*, 2008). See profiles locations in Figure 9. Note that the broad area covered by alluvium, located west of Stop 1.9 shows high frequencies that are interpreted as evidence of a magnetic basement composed by mid-Tertiary volcanic rocks. Magnetic profile 03 crosses the Ventura volcanic lineament in an area where only Mesozoic limestone is exposed on the surface; the profile does not show any evidence of a hidden dike.

Stop 1.11
Steeply dipping Joya Honda pyroclasts.

We will pass the place where the trucks are parked, and walk along the edge of the crater, to a site where the Btb2 deposit is distinctly bedded and bedding is steeply inclined (> 30°).

Studying the general structural attitude of the bedding in the pyroclastic deposit deposited north of the crater (Figure 8), and taking into account that the tephra accumulated atop a hill (see the line labeled "pre-maar surface" in Figure 12), it is obvious that, at least in part, layer inclinations were caused by the shape of the pre-maar surface. However, in other localities where this happens (*e.g.* Joya Prieta, Stop 2.4), the dip angle in the pyroclastic gradually decreases upsection. Here (22° 25' 22.67"N, 100° 47' 14.19"W) we are at the top of the pyroclastic succession and the dip angle of the bedding is considerably larger than that found in most deposits around maar craters surrounded by a tuff-ring succession (*e.g.* Wohletz and Sheridan, 1983). This is another unusual feature in the Joya Honda deposit, which makes it more similar to a tuff-cone succession (Wohletz and Sheridan, *op. cit.*)

DAY 2
Regional tectonic setting and geology of Santo Domingo volcanic field

Joya Honda has been the subject of several investigations and there is considerably more information about it. In contrast, the petrology of the volcanic rocks and the study of deep-seated inclusions has been the main focus of the research done at the Santo Domingo volcanic field. Most information about the geology of these volcanoes was obtained by Aranda-Gómez (1982) and comes from that source with the addition of a few observations made while collecting rock samples for petrology of the lavas (Luhr *et al.*, 1989; Pier *et al.*, 1989) or for the study of mantle xenoliths (Luhr and Aranda-Gómez, 1997; Dávalos-Elizondo *et al.,* 2011).

Stop 2.1
Panorama showing the regional trend of Laramide structures south of the San Tiburcio lineament.

Stop 2.2
WNW trending, plunging syncline exposed just south of La Polvora junction.

Stop 2.3
Near-vent pyroclastic succession associated to the Santo Domingo maar. Presence of kaersutite megacrysts and composite mantle xenoliths.

Highway 80 crosses the ejecta blanket of the maar. We will park the vans on the western side of the highway and we will walk a few hundred meters to the place marked in Figure 14.

The Santo Domingo maar is a small crater located 4 km northwest of the Santo Domingo village (Figure 14). It is a small (480 x 380 m), squarish, slightly elongated, depression partly excavated in limestone. Maximum height difference (140 m) between the bottom of the crater and the top of the pyroclastic succession occurs in the southwestern portion of the crater; however it is uncertain how deep the crater excavated is, as the pre-maar topography was relatively abrupt in that area. The major axis of the crater trends N45E, nearly perpendicular to the Laramide folds in the region. On the walls of the crater thick banks of the platform-forming limestone of El Abra Formation are exposed. Resting on top of the limestone is a thin ejecta blanket composed mainly of heterolithologic tuff-breccia. North of highway 80 the pyroclastic deposit is underlain by unconsolidated fluvial gravel deposit.

The following sequence is observed in the southwestern part of the crater: a thin conglomerate cemented with calcareous material (caliche?) and containing fragments of the pyroclastic rocks cover the base of the base of the pyroclastic succession. The base of the exposed section is composed of an unsorted, massive, tuff-breccia. Lapilli-sized hawaiite fragments make 85-90% of the deposit; limestone fragments tend to be larger (up to 2 m long) and make the rest of the deposit. Comminuted fragments of mantle peridotite and few xenoliths can be observed in this unit. Resting atop the massive tuff-breccia is poorly to distinctly bedded, heterolithologic tuff-breccia composed of clasts of limestone and hawaiite, with a small ammount of spinel-lherzolite and feldspathic granulite xenoliths and amphibole (kaersutite; a TiO_2-rich hornblende) xenocrysts. Compared to the tuff-breccia at the base of the succession, this unit is finer-grained and contains a larger proportion of limestone clasts. Most of the clasts are on the range of fine to coarse pebbles. Larger fragments, up to the size of small cobbles (mostly limestone), make less than 5% of the rock.

Five hundred meters west of the center of the crater, at the bottom of a small canyon, there is a very well-exposed, light yellow to white, very fine-grained tuff, which locally presents sedimentary structures

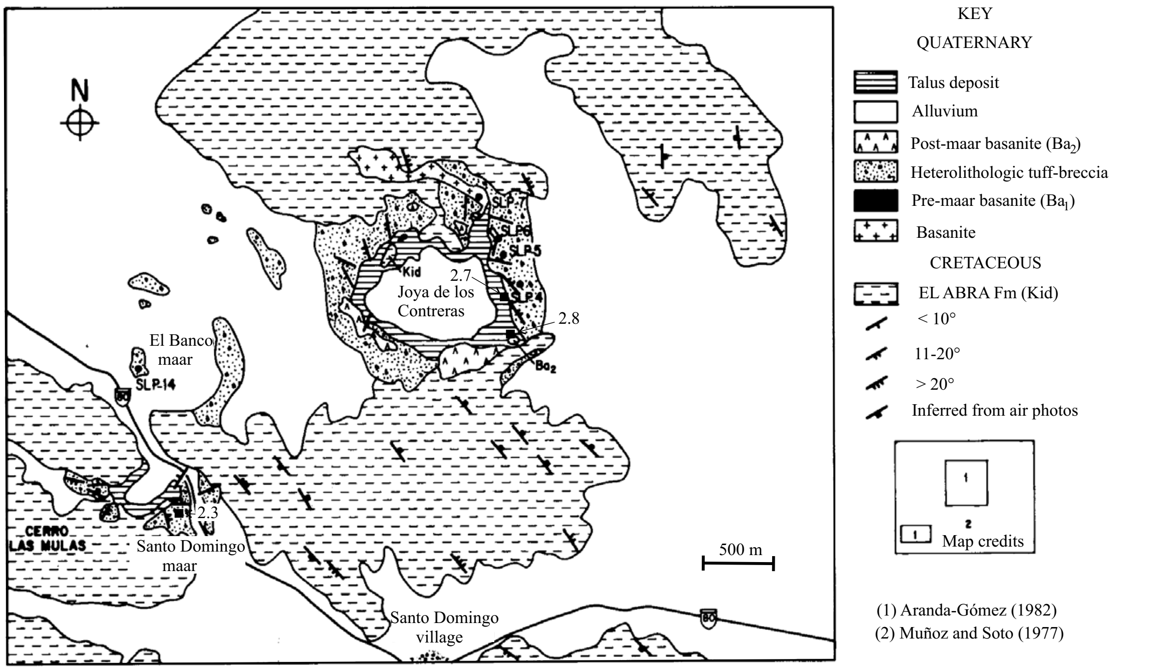

Figure 14. Geologic map of the Santo Domingo village region. Stops 2.3 and 2.4 are shown as black squares (Aranda-Gómez *et al.*, 1993)

characteristic of base-suge deposits. Resting on top of this tuff is the tuff-breccia, that we interpret as roughly equivalent to intervals 4-10 in the section studied at Joya Honda (Figure 11; Stop 1.5).

Stop 2.4
An overview of Joya Prieta. General dimensions, form and geologic setting of the maar. Observations about bleached limestone fragments. Discussion about mantle xenoliths.

Standing at 22° 56’ 52.76”N, 100° 13’ 39.74”W we will see a panoramic view of the crater, please refer to Figure 15.

This crater has a somewhat elliptical form with its major axis oriented N75E, nearly perpendicular to the Larmide folds in the pre-volcanic basement. The size of the major and minor axes is 750 and 500 m, respectively. Maximum relief from the bottom to the top of the rim is approximately 200 m in the eastern wall of the crater.

In the northern wall of the crater very thick beds of El Abra limestone are exposed. They are partially covered by a near-vent alkali basalt agglutinate and lava flow (Figures 15–17). Resting atop these pre-maar volcanic units is a pyroclastic sequence, which is dominated by a well indurated and distincly bedded, heterolithologic tuff-breccia composed of accidental fragments of country rock, juvenile clasts of alkali basalts, and a small proportion of crustal feldspathic granulites and mantle-derived ultramafic xenoliths and megacrysts. This pyroclastic sequence was produced by phreatomagmatic explosions associated with the maar formation. The attitude of the tephra beds roughly mimics the pre-maar surface, forming a pseudo-fold caused by the initial, depositional, bedding in the surge beds. In the southern rim of the crater the volcanic sequence is absent, probably caused by northerly-directed phreatomagmatic blasts. A portion of a Laramide structure, with a fold width in the order several kilometers, is exposed on the southern wall of the maar. The hinge zone of the structure occurs in the crater area. Structural data compiled and analyzed by Aranda-Gómez *et al.* (2000) indicates that the structure is a symmetric open fold with a near-vertical axial plane trending N71W.

The excavation of the maar crater was preceded by strombolian activity that formed a basaltic agglomerate. This unit can be seen resting on top of the limestone in several places around the crater. The tuff-breccia formed by phreatomagmatic activity is underlain by a finer-grained tuff. Resting on top of the tuff is a heterolithologic tuff-breccia characterized by the absence of ultramafic xenoliths and kaersutite megacrysts. The hawaiite clasts in this unit are oxidized. The uppermost part of the succession is a heterolithogic tuff-breccia with abundant megacrysts of kaersutite and xenoliths. This unit forms the bulk of the ejecta blanket and can be seen almost continuously around the crater. A thin tuff deposit separates the lower tuff breccia from the uppermost xenolith-bearing deposit, which is relatively rich in primary clasts (compared with other maars visited in this field trip). Depending upon their diameter, limestone clasts are partially to completely bleached. The unit ranges from faintly to distinctly bedded and bed thickness ranges from 0.3 to

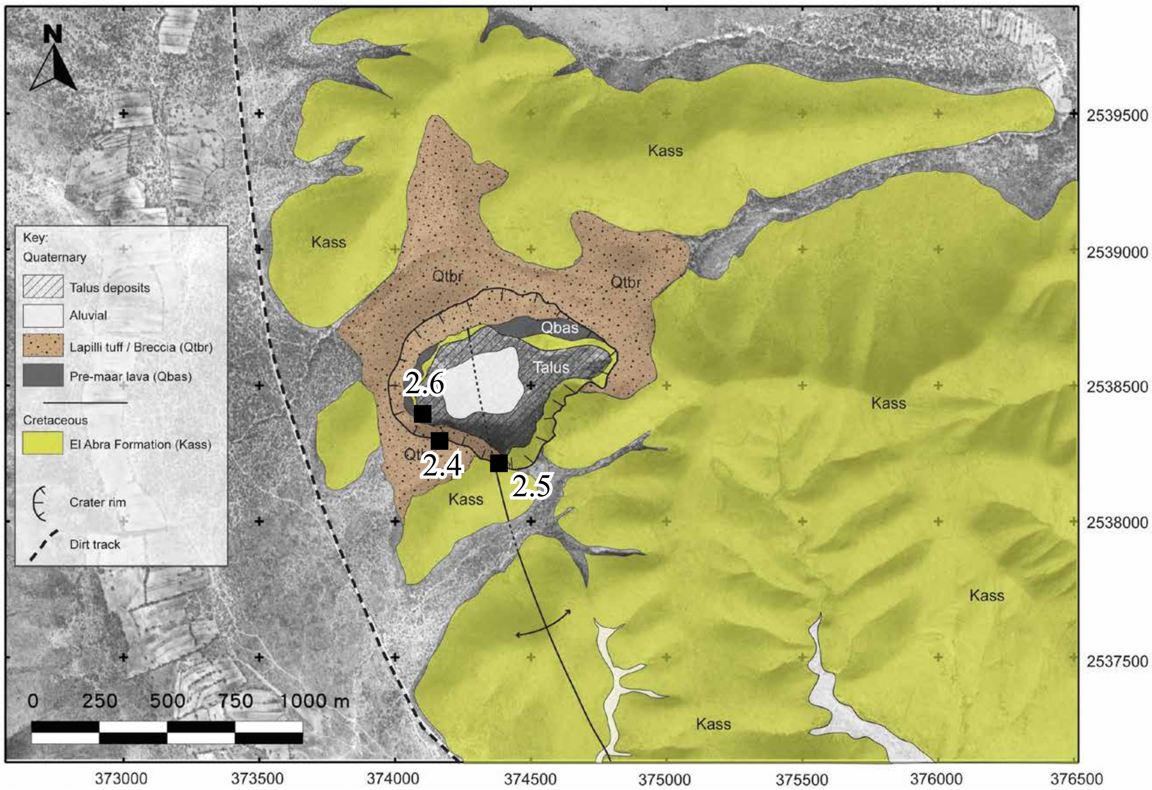

Figure 15. Geologic map of Joya Prieta.

1.0 m. The clast range from 12 to 0.5 cm. Most fragments are around 8 mm in diameter. A rough visual estimate of the composition of this rock is: limestone clasts 5 to 7%, juvenile clasts 10 to 15%, kaersutite megacrysts 1% and matrix formed by comminuted limestone and hawaiite 75-80%. The medium brown coloration of the rock suggests that juvenile material is the main constituent of the matrix.

In the northern wall of the crater the limestone is overlain by a massive volcanic agglomerate composed of oxidized scoria. That unit grades upward to a better sorted, faintly stratified lapilli tuff composed of scoria. Resting atop the lapilli tuff is a fine grained, cross bedded tuff interpreted as a surge dominated deposit. Above this is the xenolith-bearing tuff-breccia.

Many limestone fragments within the tuff-breccia are partly to completely bleached. This feature is not present in the pyroclastic deposits associated to the Ventura – Espíritu Santo maars. We speculate that this feature may be related to a higher temperature of emplacement of the surge deposits in the Santo Domingo volcanoes.

One of the most striking characteristics of the Santo Domingo volcanic field maars is the presence of rare composite xenoliths; in a single xenolith foliated lherzolite is in sharp contact with hornblende pyroxenite, which proves the mantle origin of the kaersutite. Many lherzolite xenoliths display a weak foliation and segregation banding, as well as bimodal grain size. Orthopyroxene porphyroclasts (up to 5 mm long) are surrounded by a relatively coarse-grained groundmass made of olivine, unstrained, equant neoblasts (1-2 mm in diameter). Most peridotites in the Santo Domingo volcanic field are tectonites from the mantle. These features, together with the marked change in the trend of the Laramide structures along the lineament where the volcanoes are located, and evidence of recurrence of volcanism along the lineament, make us believe that there could be an important basement structure concealed under the Mesozoic sediments.

Stop 2.5
Fracture filled with calcite. Is this evidence of circulation of ground water in open fractures?

We will follow for a short distance a narrow trail that begins at 22° 56’ 50.90”N, 100° 13’ 33.43”W. Along the trail part of the pyroclastic succession described in Stop 2.4 is exposed

At the beginning of the trail thick beds of El Abra limestone are exposed . In this region the limestone is dominated by lagoonal facies accumulated well into the Valles – San Luis Potosí calcareous platform. Facies variations observed in the limestone suggest the presence of isolated patch reefs in the area.

As it was shown in Joya Honda (Figure 12), it is clear that the pre-maar surface in this area was also composed of hills and fluvial valleys, and there is no

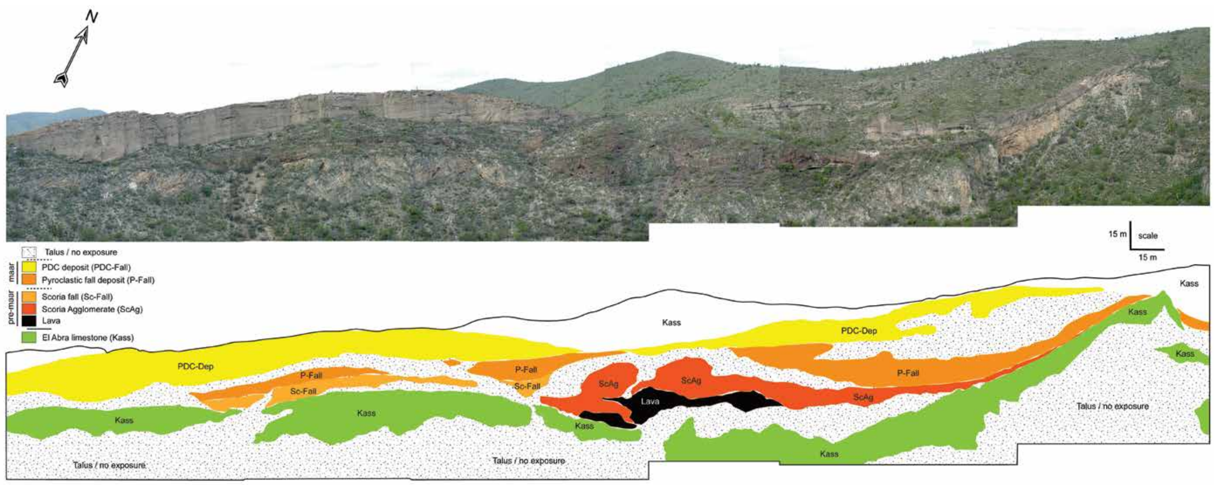

Figure 16. Panoramic view with stratigraphic interpretation of the deposits of Joya Prieta´s northern wall.

evidence in the crater's walls of the presence of a clastic deposit where a darcian aquifer could be hosted. Therefore, groundwater must come from fractures or conduits within the limestone. The presence of this fracture, filled with calcite precipitated in an open space, supports our interpretation about the nature of aquifer in some of these maars. It is worth stressing that our reconnaissance work in the immediate surroundings of the crater failed to show the presence of large karstic features such as sinkholes. However, in almost any surface on the limestone there are a plethora of small scale dissolution features.

Stop 2.6 Pre-maar lava flow exposed on the western wall of the crater. Changes in water/magma ratio

A few tens of meters below the location of Stop 2.4 a small intra-canyon lava flow is exposed. This unit was formed during the early stages of the maar-forming eruption. We believe that the formation of Joya Prieta started with a dry eruption, that changed to hydromagmatic activity when ground water contained in fractures within the limestone entered into contact with the magma. Here the change from dry to wet eruption is more evident than in Joya Honda, where the increase in water content in the system is based on the interpretation of the base surge exposed in intervals 4 -10 (Figure 11) was produced by relatively dry explosions.

Stop 2.7
An overview of Joya de los Contreras tuff-ring and a quick look to the base of the pyroclastic sequence on the eastern wall of the pyroclastic deposit

This volcano is located 3 km north of the Village of Santo Domingo. We will follow a dirt road that winds around a small limestone mountain located immediately north of highway 80 until we reach the eastern border of the crater. Our first stop is at 22° 53' 33.83"N, 100° 16' 37.69"W and we will walk along the base of the pyroclastic deposit toward 22° 53' 42.09"N, 100° 16' 39.88"W

Joya de los Contreras is a large shallow crater of roughly elliptical form, surrounded by an ejecta blanket that is in some places 75 to 100 m thick. The major axis of the crater is 1,400 m long and trends E-W. The minor axis is 980 m long. The bottom of the crater is 40 m below the adjacent alluvial valleys located immediately east and west of the crater.

The volcanic activity in this crater seems to have started north of the crater with the formation of a small intracanyon lava flow. Contemporaneous (?) with this flow, in the place now occupied by the crater, one (or several?) scoria cone formed a basaltic agglomerate (Ba_1 in Figure 14). This agglomerate may be clearly seen in places below the pyroclasts deposited during the maar-forming eruption. After the phreatomagmatic phase of the volcanic complex small eruptions of mafic lavas formed relatively thin agglomerates (Ba_2) in several places around the crater.

The lowermost agglomerate (Ba_1) is composed of highly vesicular, glassy fragments of hawaiite. Limestone fragments are generally absent in this unit. The size of the juvenile fragments ranges from 0.5 to 50 cm. The glassy material is highly oxidized and has a reddish brown color. Mantle peridotite xenoliths are common in this unit.

Resting atop of Ba_1 is a pyroclastic succession formed by a faintly to distinctly bedded tuff-breccia interlayered with some beds of heterolithologic tuff. The pyroclasts are formed by a mixture of limestone and hawaiite fragments and some xenoliths of mantle peridotites and lower crust granulites. The pyroclastic deposit is formed by layers up to 50 cm thick and each bed displays internal laminations. The bedding is generally parallel but in some places low angle cross

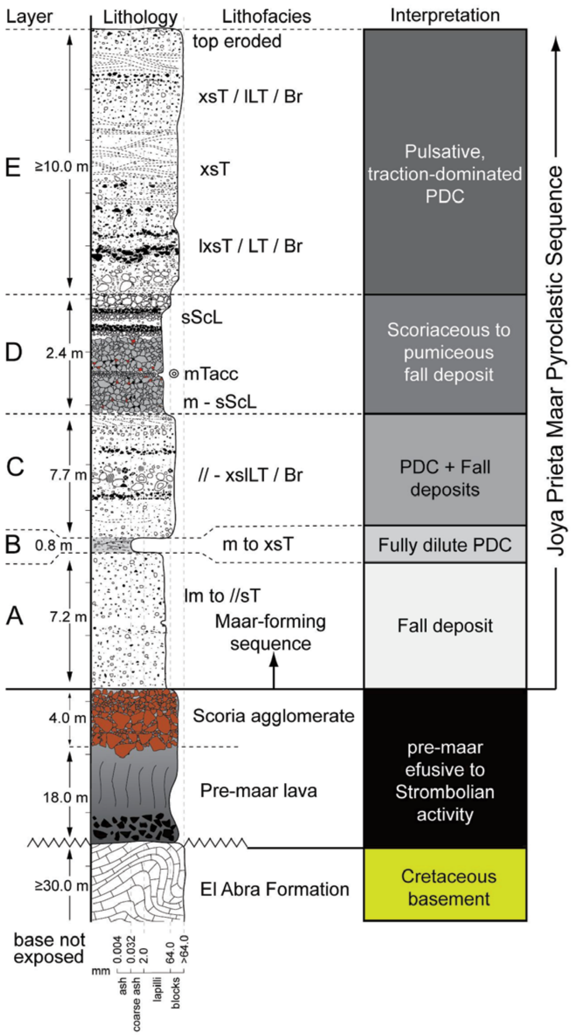

Figure 17. Generalized vertical stratigraphy of Joya Prieta tuff-ring. Modified from Dávila-Harris (2003).

stratification may be found. The pyroclasts range in size from volcanic dust to blocks up to 30 or 40 cm long. The most common fragment size is 0.5 to 1 cm long. Larger clasts form 5 to 10% of the deposit. The fragments in the tuff-breccia range from sub-angular to rounded. Xenoliths tend to have roughly tabular form with the edges slightly rounded. The matrix of the tuff-breccia is composed of dust-sized juvenile material and comminuted limestone. Small lateral variations in the lithology and in the bedding type are common in the deposit.

Fine grained, heterolithologic tuffs with sedimentary structures that suggest that they were accumulated from surges occur in several places. Their stratigraphic position within the pyroclastic succession varies from place to place.

It is worth mentioning that kaersutite megacrysts, are scarce (as compared with the Santo Domingo maar and Joya Prieta). Those found at Joya de los Contreras occur in the upper part of the tuff-breccia.

Stop 2.8
Post-maar vent. Are these features controlled by the buried diatreme-country rock contact?

We will walk a short distance to see one of the post-maar agglomerates at 22° 53’ 27.22”N, 100° 16’ 40.05”W.

Post-maar mafic agglomerates (Ba_2) can be seen in several places around the crater’s rim. Their spatial distribution suggests that they were fed through the ring-fault that marks the hidden diatreme-country rock contact. The agglomerates are in general chaotic and unsorted. The hawaiite fragments are highly vesicular, glassy and oxidized. Their size ranges from 1 or 2 cm to 2 to 3 m. Limestone fragments are rare. Abundant xenoliths are always present in the agglomerate.

A final comment about Joya de los Contreras: We believe that this is a somewhat unusual maar as pre-maar rocks (gravel deposits made of limestone clasts) are not obvious beneath the maar- related pyroclastic succession. However, the height difference between the bottom of the crater and the adjacent, alluvium filled valleys is significant (40 m). Thus, the crater was excavated below the pre-maar surface. It is not clear if part of the hills made of El Abra limestone were blasted or not. Likewise, it is possible that shallow water might have been included in the calcareous gravel deposit. In our experience, it is unusual for post-maar vents to be located around the crater rim. It is more common to find the post-maar vents near the center of the crater, as it happens in La Breña (Aranda-Gómez *et al.*, 1992), and in Hoya Blanca and Hoya Cíntora in the Valle de Santiago region. Kaersutite crystals appear to have arrived to the surface late in the phreatomagmatic phase of the complex. We have similar occurrences where xenoliths and xenocrysts appear to be restricted to a portion of a stratigraphic sequence in a scoria cone (Cerro Santa María), or a given lava flow (Cerro El Toro) in the western portion of the Ventura – Espíritu Santo volcanic field.

We also note that the elongation of this crater appears to be independent of the orientation of the local Laramide structures in the area, which trend N60W. However, as far as we can see, the crater for the most part grew in clastic deposit, not in layered limestone. We also speculate that the crater’s growth may have been arrested by the neighboring limestone hills and by the system running out of water at the closing phase of the eruption.

DAY 3

Geology of La Joyuela tuff-ring. A second visit to Joya Honda and final discussion about the influence of country rock on the shape of maar craters in deformed limestone.

On the last day of our field trip, we will go back to the Ventura – Espíritu Santo maars to study an elliptical tuff-ring. We will also make a brief visit to the only maar in the area that has a nearly circular form in map view. At the end of the day, if time allows it, we will go back to the SW edge of Joya Honda to have a final discussion about the role anisotropies in the country rock may play in the shape of the craters excavated in folded limestone. Our intention is to get to Querétaro on time to assist to the icebreaker cocktail.

Stop 3.1
An overview of the Laguna de los Palau maar. Dimensions, shape and nature of the pre-maar rocks exposed on the crater's walls. Was the aquifer of the darcian type and if so, what was its influence on the form of the maar?

This maar is located 35 km NE of the city of San Luis Potosí, close to the small village of Armadillo. The volcano is on the eastern side of Sierra de Álvarez (Figure 5), in a region where platform sediments of El Abra limestone occur. There exist small remnants of mid-Tertiary ignimbrites in the area, and the morphology of the eastern flank of Sierra de Álvarez suggests recent uplift or change of base-level in the fluvial system (?), as the arroyos are dissecting an area formerly occupied by "bajada" deposits.

Standing at 22° 12' 50.77"N, 100° 37' 54.47"W we will see a panoramic view of the crater. The first thing that is obvious is that the morphology of the crater is completely different than that observed in the other maars of San Luis Potosí. The nearly vertical scarps observed in the pyroclastic deposits of Joya Honda and Joya Prieta are absent in this maar. Instead, the inner slopes in the crater are gently inclined toward the center of the maar. A marked change in the vegetation and presence of soils is also evident. Whether this is related to an obvious change in the prevailing climate in this region as compared to the other places where the rest of the maars are located, or to a combination of climate and nature of the pyroclastic deposit, remains to be documented.

The crater is nearly circular (Figure 18), with an approximate diameter of 1,400 m and maximum height of the tephra ring close to 60 m. The volcanic sequence rests on top of a continental gravel deposit with an inferred Plio-Quaternary age (?). The gravels are underlain by folded Mesozoic marine sediments. Close to the crater crop out rocks of El Abra, Soyatal and Cárdenas formations. Mid-Tertiary felsic volcanic rocks are exposed a short distance east of the crater.

The pre-maar sequence exposed inside the crater is composed of very poorly stratified and sorted gravel and sand deposits. Clast sizes range from fine pebbles

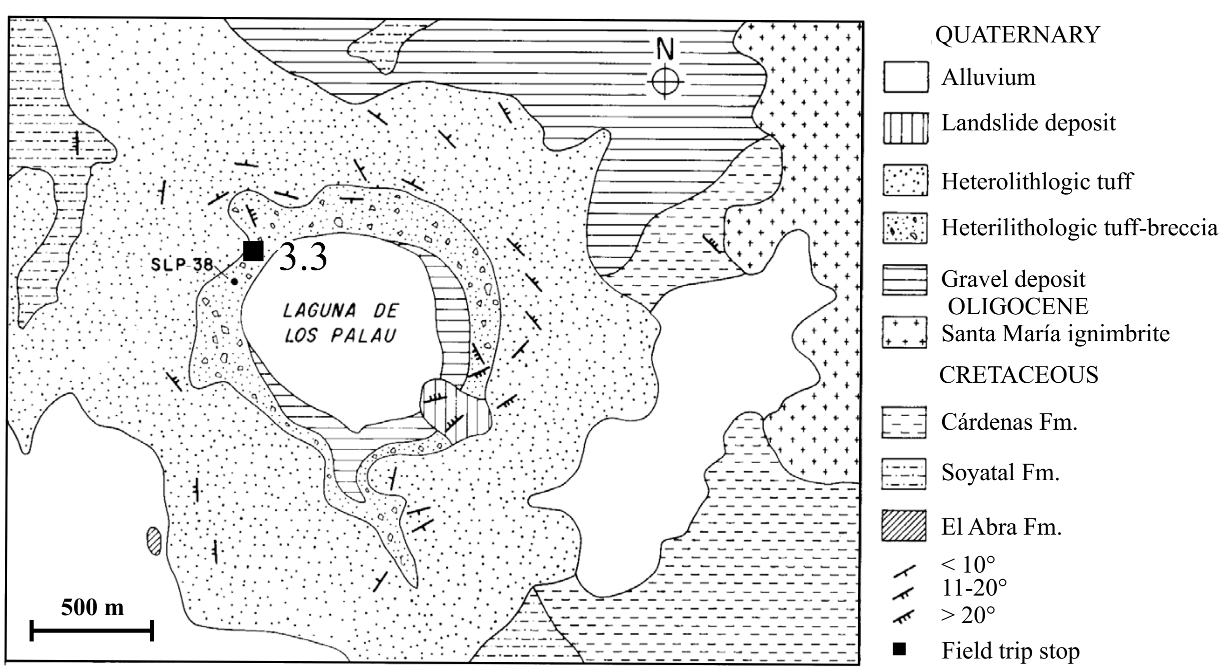

Figure 18. Geologic map of Laguna de los Palau (Aranda-Gómez *et al.*, 1993).

to large boulders. The matrix is formed by sand and silt-sized clasts. The clasts are mainly limestone and chert fragments derived from the marine sediments exposed in Sierra de Álvarez. Well-rounded, intensely weathered, boulders of felsic volcanic rocks are also common in the deposit. The matrix is strongly cemented with calcite.

The maar-related pyroclastic succession is very poorly exposed in the crater. The inner part of the maar is covered by soil. The outer part is concealed by abundant caliche. Almost all the information about the pyroclastic succession comes from an area in the SE portion of the crater. Unfortunately, that area was modified by a landslide, making the interpretation of the succession difficult.

Aranda-Gómez (1982) recognized several lithological units. Resting atop the gravel deposit is a coarse grained, tan color tuff, which in places has sedimentary structures such as channels, low angle cross-stratification, and antidunes, that he interpreted as deposited by pyroclastic surges. A heterolithologic tuff-breccia is sometimes exposed in the walls of the crater. This unit may rest directly on top of the pre-maar gravels or on the surge deposit. The tuff-breccia is massive to poorly stratified. It is composed of limestone fragments and mafic volcanic rock, up to 10 cm in diameter. The matrix is formed by lapilli- and volcanic dust-sized fragments of the country rock and juvenile ejecta. Mantle and lower crust xenoliths, generally coated with basanite are common. The tuff-breccia grades upward to a heterolithologic lapilli tuff, which extends several hundred meters away from the crater edge (Figure 18).

Stop 3.2
An overview of the geology of La Joyuela. Dimensions, shape, and its relation with the Ventura volcanic lineament. Is this a maar (*sensu stricto*) or a tuff-ring?

Standing on 22° 21' 56.30"N, 100° 46' 57.56"W we will see a panoramic view of the inner part of the crater, similar to that shown in Figure 19.

This volcano is located at the intersection of the Ventura volcanic lineament with an ENE-trending, right-lateral fault that displaces the Laramide folds (Figure 5). The crater is elliptical, with its major axis trending N70E, perpendicular to the Laramide folds in the area, and roughly parallel to the right-lateral fault, between Sierra de Álvarez and Sierra del Coro (Figure 5). The form and orientation of the crater with respect to these structures suggest that structural control played an important role in the formation of the maar. However, it must be noted that the Ventura volcanic lineament is perpendicular to the major axis of the crater. The sizes of the major and minor axes are 1500 and 700 m, respectively. The crater is surrounded by an almost continuous rim or pyroclasts (Figure 20). The maximum height of the rim is 80 m in the northeastern wall. The tephra deposit thins out toward the W and disappears in the SW part of the crater (Figure 20). The pyroclastic ring is not continuous due to wedging-out of the deposit and to erosion caused by several small arroyos that discharge inside the crater. Inside of the crater, at the base of the SE wall is exposed Cretaceous limestone (Kip in Figures 18 and 19). However, compared with Joya Honda and Joya Prieta, the crater is relatively shallow, making this volcano more similar to a tuff-ring.

Several volcanic vents of varying age are closely related with La Joyuela.. The geologic map of the crater suggests that the zone now occupied by the crater was covered by a lava flow (B1 in Figures 19 and 20). Thickness variations in the B1 unit indicate that it originated in a small scoria cone exposed in the southeastern portion of La Joyuela (U locality in Figure 19). The eruption of B1 seems to have been followed by formation of a small scoria cone now exposed in the northeastern wall of the crater (Figure 19, locality S).

The maar-forming eruption followed the formation of the spatter cone Ba_1, and it began with the accumulation of a mafic agglomerate (Ba_2 in Figure 19). Thus, the initial phase of formation was dominated by strombolian activity, which later changed to phreatomagmatic explosions. The pyroclastic succession accumulated during the hydrovolcanic stage is xenolith-bearing, heterolithologic tuff-breccia (Btb in

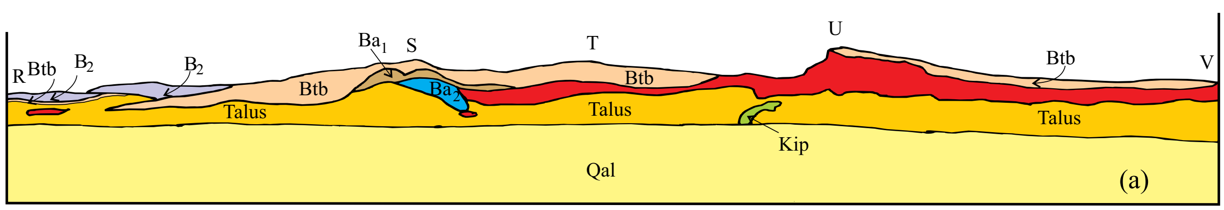

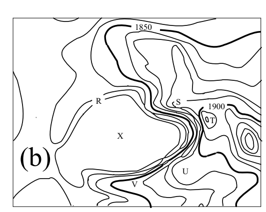

Figure 19. (a) Geologic sketch map of t he eastern wall of La Joyuela tuff-ring. Units figured are: Kip= Cretaceous limestone; Ba and Ba = Mafic agglomerates; Btb = Heterolithologic tuff-breccia; B = pre-maar "basalt" (olivine nephelinite) and B = post-maar "basalt". (B) Topographic map of the crater area. Points R, S, T, U, and V show approximate location of the respective points labeled in the sketch. X is the point from which photographs used to make the sketch were taken. (Aranda-Gómez, 1982)

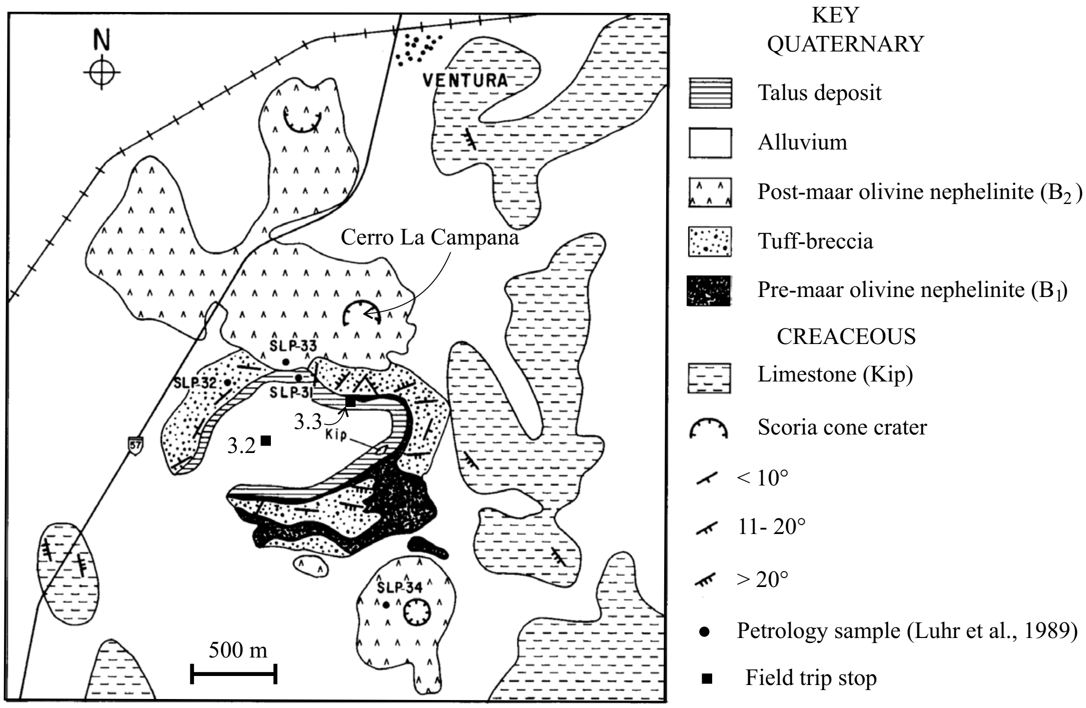

Figure 20. Geologic map of La Joyuela (Aranda-Gómez *et al.*, 1993).

Figure 19). This deposit ranges from massive to distinctly bedded. Layers are 50 to 60 cm thick and commonly present internal laminations with low angle-cross bedding and graded bedding. The tuff-breccia is composed of blocks of limestone and olivine nephelinite set in an unsorted matrix of volcanic dust and comminuted country rock. Accidental rock fragments of a salmon-pink, felsic volcanic rock are sometimes seen in the deposit. Xenoliths of peridotites, pyroxenites and feldspathic granulites occur throughout the deposit.

A thin lava flow of olivine nephelinite, originated at the nearby La Campana scoria cone (Figure 20), rests on top of the tuff-breccia in the northern part of the crater (point R, Figure 19). Relatively abundant xenoliths occur close to the base of that lava flow.

Stop 3.3
Pyroclastic stratigraphy and general eruptive history of La Joyuela volcano from its pyroclastic deposits exposed at the northern wall.

We will drive (or walk) into the crater floor and hike uphill towards the pre-maar agglomerate and phreatomagmatic fall and flow deposits that represent the maar-forming sequence. ¡Be aware of wasps nests at the crater walls!

A detailed stratigraphic account (Figure 21)from La Joyuela maar pyroclastic sequence has been done by Dávila Harris (2003), the description presented here is a synthesized version of that study.

The La Joyuela volcanic sequence was divided in three informal members (Figure 21): I, II and III, each one representing distinct lithological and genetic features, and each member has been sub-divided into several units from A to O (Figure 21).

Member I. It has been sub-divided in units A to D. It is a 28 m thick succession of lava flows, spatter agglomerate and scoria blocky breccia deposits. It is regarded as a pre-maar lava sequence. From the base to top, it is formed by: A) A 6 m thick, massive basanitic lava flow; B) Spatter agglomerate of approximately 4 m thick, monolithologic, massive and very poorly sorted, containing >30 cm blocks and bombs; C) A second spatter agglutinate, thicker than previous one (aprox. 16 m thick), relatively better sorted and oxidized; D) It is a 2 m thick volcanic blocky breccia probably from a lava front, with pervasive palagonitization, probably due to the first stages of hydrovolcanism, the deposit overlies gradually unit C and grades into the overlying unit.

Member II. it is represented by approximately 7 m of well-stratified pyroclastic fall deposits subdivided from E to F units described below. It marks the transition between “dry” eruptions and the beginning of phreatomagmatism. Unit E: 1.8 m thick, well-stratified fall deposit, lapilli-sized formed by juvenile clasts. Unit F: a 4.5 m thick layer of massive to stratified tuffs, probably from fallout origin with scattered laminated ash layers. The deposit is formed mainly by juvenile and limestone clasts, with a low percentage of free phenocrysts. Unit G: Stratified layer 0.9 m thick, well indurated, with slight inverse grading with a thin ash-layer towards the top.

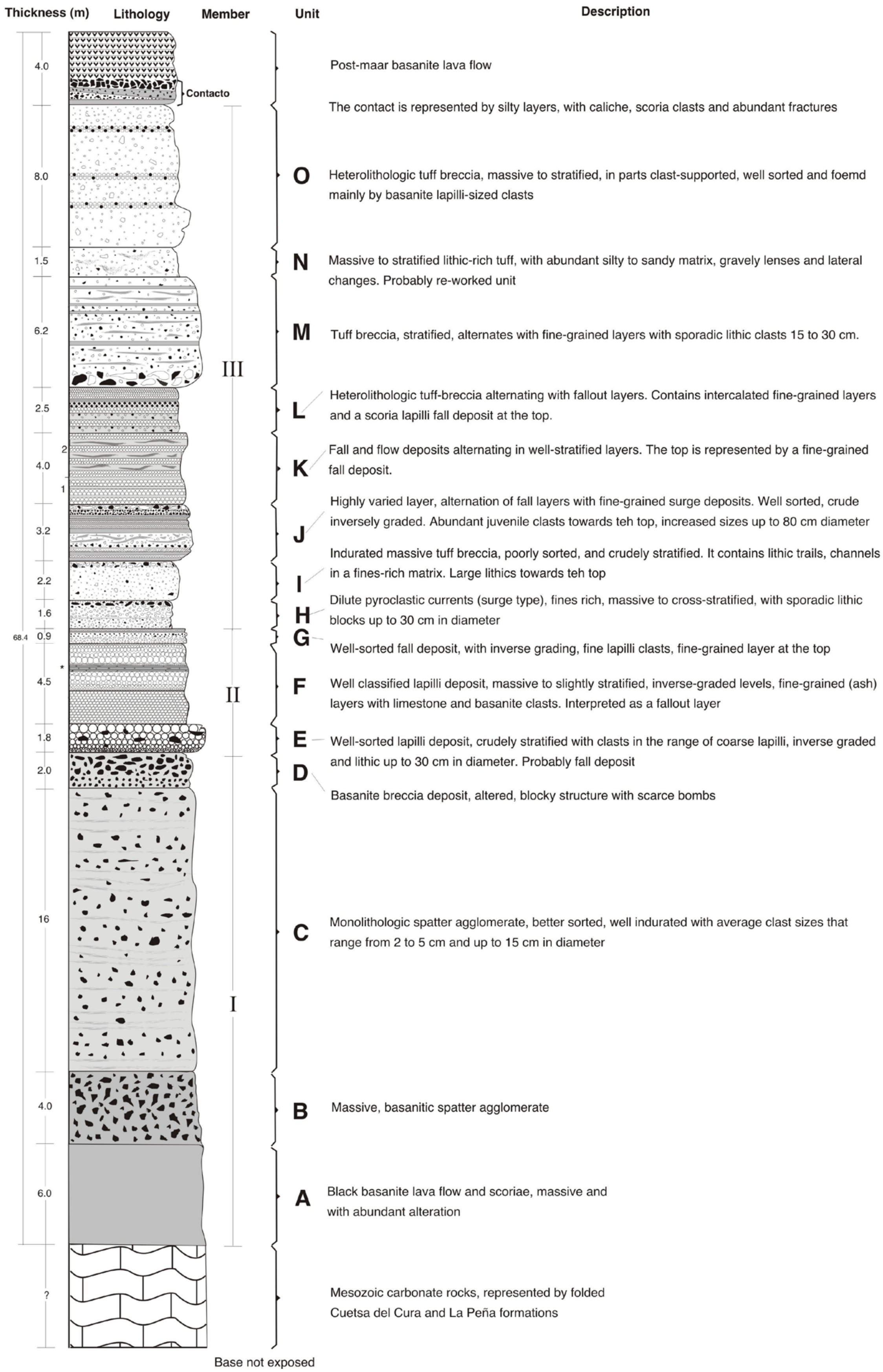

Figure 21. General vertical stratigraphy of La Joyuela tuff-ring.

Member III. It represents the top and thickest member and it is formed mainly by a well-indurated pyroclastic lithic tuff-breccia sequence 30 m thick. It has been sub-divided into 8 layers (units H to O), that probably represent the maar-forming sequence. This classification was made in order to improve and ease the understanding of the succession as well as to identify vertical changes and correlation across the structure. Unit H: It is a 1.6 m massive, heterolithologic tuff-breccia. It is poorly sorted, matrix supported tuff with blocks up to 60 cm in diameter. Unit I: It is a 2.2 m tuff breccia, with more sedimentary structures than unit H, it presents subtle inverse grading with accumulation of lithic trails. Few blocks within this layer present prismatic joints. Unit J: a 3.2 m thick layer with abundant textural and sedimentary variations. It contains clast-supported lapilli layers interlayered with massive to stratified lithic-rich layers of basanite clasts more than limestone and calcareous shale lithics. Few lithic blocks exceed 80 cm in diameter. Unit K: it is a 4 m thick alternation of stratified “surge type” layers, with cross-stratified domains and alternation of lapilli fallout deposits. Towards the top the deposits is fines-rich although with other clast-supported fallout layers. Unit L: Heterolithologic tuff breccia 2.5 m thick with intercalated lapilli fallout layers. The deposit here is fines-rich, not as indurated as previous facies. It shows undulated stratification, deformed layers and probably convoluted stratification, although no other evidences of moist conditions have been recorded. Unit M: Stratified succession of tuff-breccias with almost 6.2 m thick, normal graded in a fines-rich matrix Unit N: 1.5 m thick massive, lithic-rich deposit. It contains lenses of lithic material in a silty to sandy matrix. It has been interpreted as a probably re-worked layer at the last stages of the eruption. Unit O: Heterolithologic breccia with an approximate thickness of 8 meters. It contains sporadic fallout lapilli layers, it resembles a crude stratification and it contains lithic clasts as large as 30 cm in a fine-grained matrix. It has been interpreted as a last stage of pyroclastic flow deposits with discrete fall deposits. The top of the pyroclastic sequence is unconformably covered by a basanite lava over a silty poorly exposed and developed paleosol.

Stop 3.4 (optional)
The SW part of Joya Honda’s crater. The role of mass-waisting on the growth of the crater

We will go back to Joya Honda, to the southwestern part of the crater, at 22° 24’ 50.88”N, 100° 47’ 28.69”W, where we can see the effects of the hydrovolcanic blasts on the pre-maar rocks exposed along a trail that leads to the crater’s interior. In our way to the crater, we will drive through a broad, flat area, covered by alluvium located west of the maar. Near the small village of La Tinaja we will pass outcrops of mid-Tertiary, felsic volcanic rocks.

Here (22° 24’ 54.27”N, 100° 47’ 31.70”W) we can see that the limestone beds cut by the maar-forming eruption form an array that resembles a set of stairs, as the beds have a SW dip, while the crater wall is steeply inclined toward the NE. This array contrast sharply with the ENE portion of the crater, where both, layers and crater wall, are steeply inclined toward the SW. We note that the relation between crater’s wall and dip of the layers in the ENE portion of the crater is ideal for the continuous development of rock slides. Likewise, we believe this phenomenon must have happened even as the crater was being excavated by the hydrovolcanic blasts. The end result of mass-wasting at the time of eruption was that the crater must have grow faster in the ENE direction than in any other direction. Figure 22 illustrates the influence of structural attitude of bedding in the limestone in the growth of the crater and in the formation of a slight asymmetry (Figure 23) in the inferred form of the hidden diatreme beneath Joya Honda (López-Loera *et al.*, 2008).

The next topic we want to discuss is also about the elliptical form of the crater and its nearly perfect match with the Laramide structures. Detailed structural work performed in the limestone is described as follows by Aranda-Gómez *et al.*(2000): “A data set composed of 130 readings of bedding plane attitudes was compiled along a ~1000 m long traverse adjacent to the southern rim of the...crater. Measurements were made approximately every 10 m, except where small, second order folds were clearly exposed. In those places... attitude readings were more closely spaced, in order to characterize the overall shape of the secondary structures. Contoured equal area lower hemisphere plots of the poles to bedding are shown in Figure [25]a-d. The whole data set (Figure [25] a) defines a girdle with the pi pole (trend and plunge of the fold axis) located at ~339/01. The presence of several concentrations of poles along the girdle, and the clear association in the field of the secondary folds with the thinly bedded strata is interpreted as evidence of disharmonic folding in the area (Figure [25]). To evaluate the significance of the pole clusters along the girdle in Figure [25]a, the data set was divided into three subsets based on field observations. Figures [25] b and [25]c represent bedding plane attitudes measured at second order folds with fold widths in the order of one to 3 m. Figure [25]d depicts the whole data set after filtering out the readings corresponding to second order folds. Inspection of Figures [25]a-d suggests that data points which define the pole clusters around 206/53 and 093/60 (Figure [25]b), and 255/18 and 270/60 (Figure [25]c) correspond to the limbs of the second order folds. The pole clusters around 070/45 and 070/07 (Figures [25]a and [25]d) coincide with the limbs of major folds exposed in the walls of the crater”.

Comparing the results of the structural analysis with the trend of the major axis of the elliptical crater, it is found that the axial plane of the folds is perpendicular to the major axis of the fold. Is it possible that

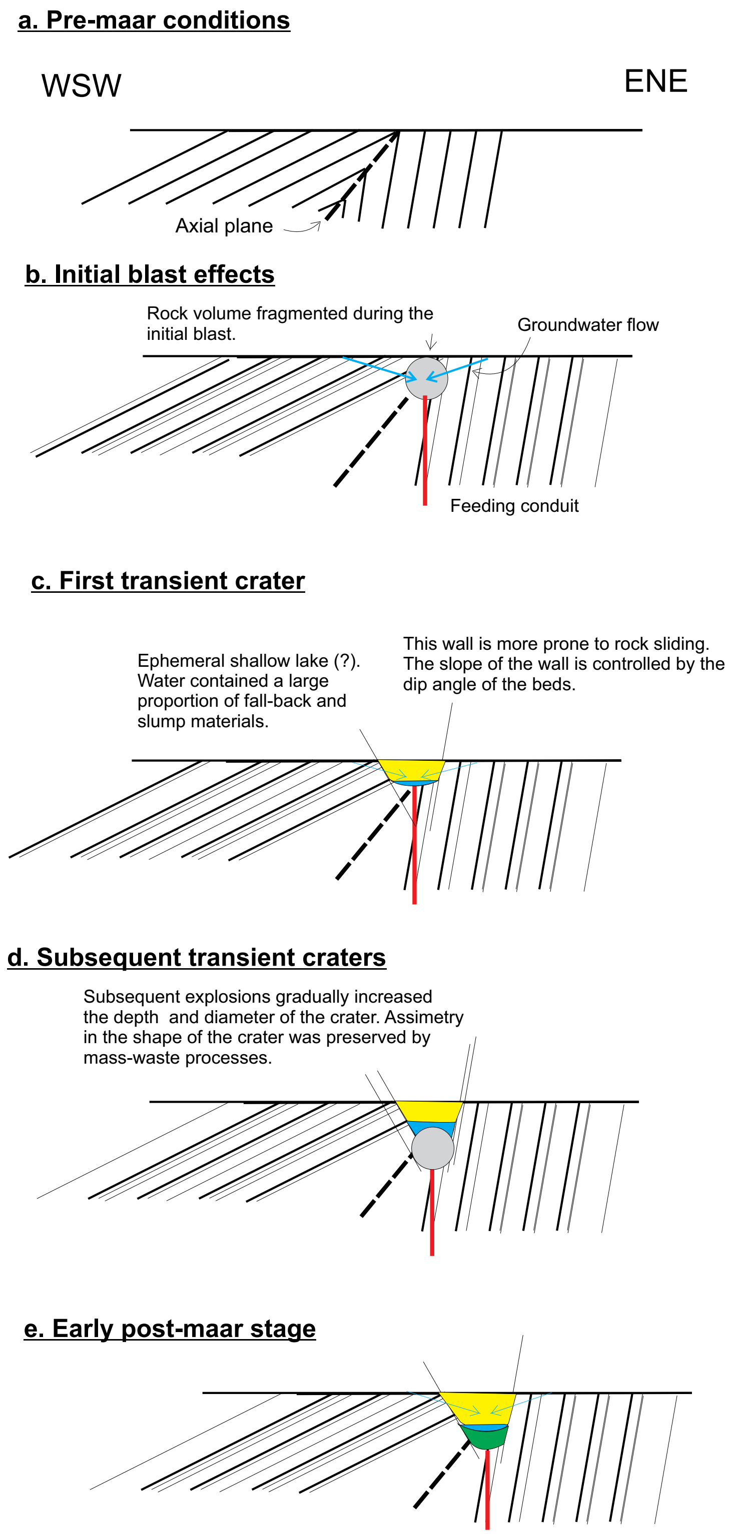

Figure 22. Conceptual model proposed by López-Loera *et al.* (2008) to explain the asymmetry of the inferred rock body (Figure 24) underneath the crater of the Joya Honda maar. The shape of the body is attributed in part to the structural attitude of the folded Cretaceous limestone. (a) Conditions prior to phreatomagmatic activity. Pre-maar relief is eliminated, and number of bedding planes is considerably reduced for simplicity. (b) The initial phreatomagmatic blasts occurred near the surface, fracturing rocks around the focus of the explosions. Fine-grained pyroclasts were ejected through open fractures producing the base surge tuff (intervals 4-10, Figure 11) (c) Mass-waste modification of the first transient crater produced by rock slides in the northeastern portion of the system. (d) As the eruption continued, magma-water interactions occurred between shallow muddy lakes at the bottom of the transient craters. Deepening of the explosion foci was very slow and independent of the formation of a cone of depression in the aquifer. (e) After the end of eruption, a lake formed and preferential mass-wasting continued, always influenced by the pre-maar structure. Later, local hydrologic conditions changed and the lake finally dried out. Lake sediments were covered by material eroded from the inner part of the crater. The final result is an asymmetric crater with a steep, nearly vertical wall in the eastern side.

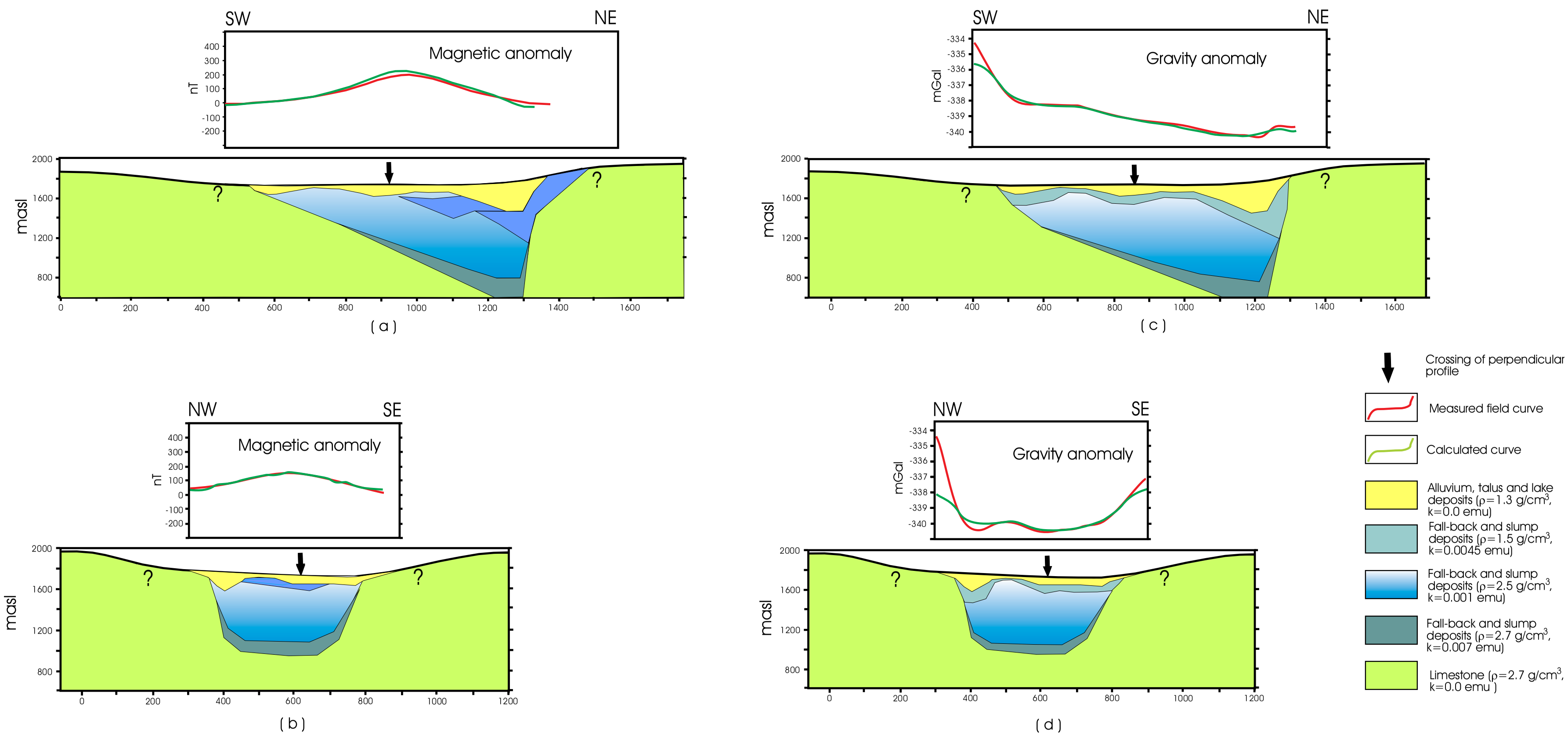

Figure 23. Magnetic and gravimetric models of the structure underneath the Joya Honda crater (López-Loera *et al.*, 2008). (a) and (b) gravimetric (c) and (d) magnetic data collected along two nearly orthogonal profiles roughly parallel to major and minor axes of the crater. The combination of an irregular body composed by post-eruptive (alluvium, talus and lake) sediments with irregular layers of fall-back pyroclastic and slump material produces a close match of both the residual magnetic (a and b) and gravity anomalies (c and d) along both profiles. Note that vertical and horizontal scales are different in all diagrams

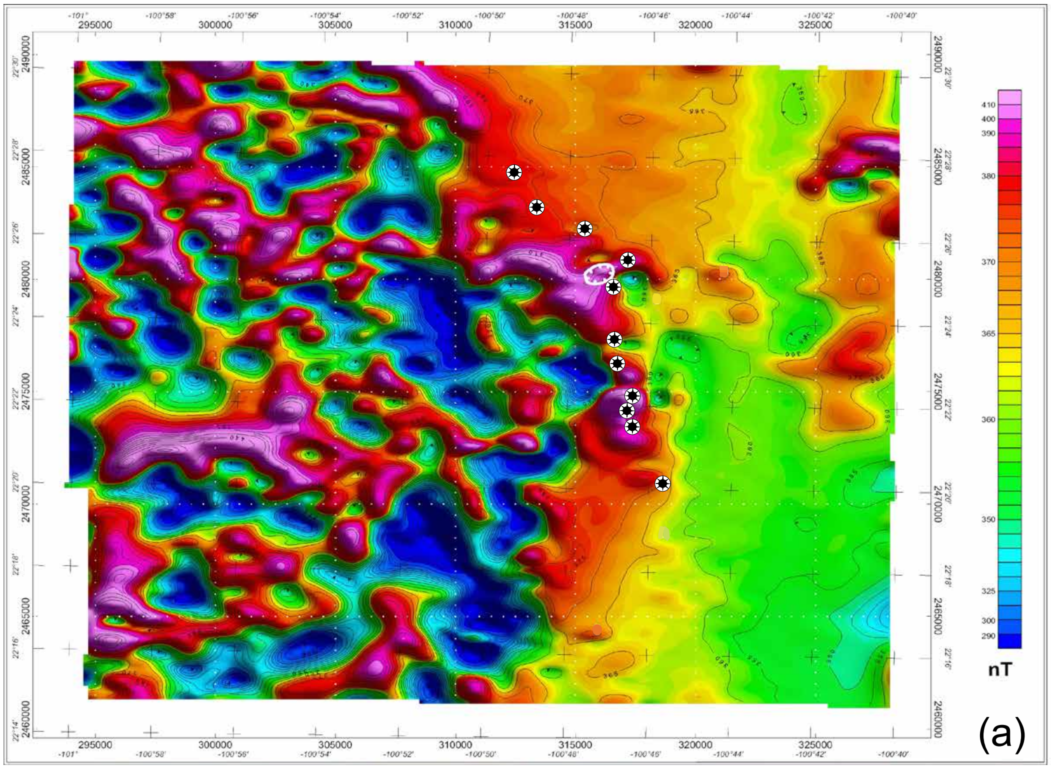

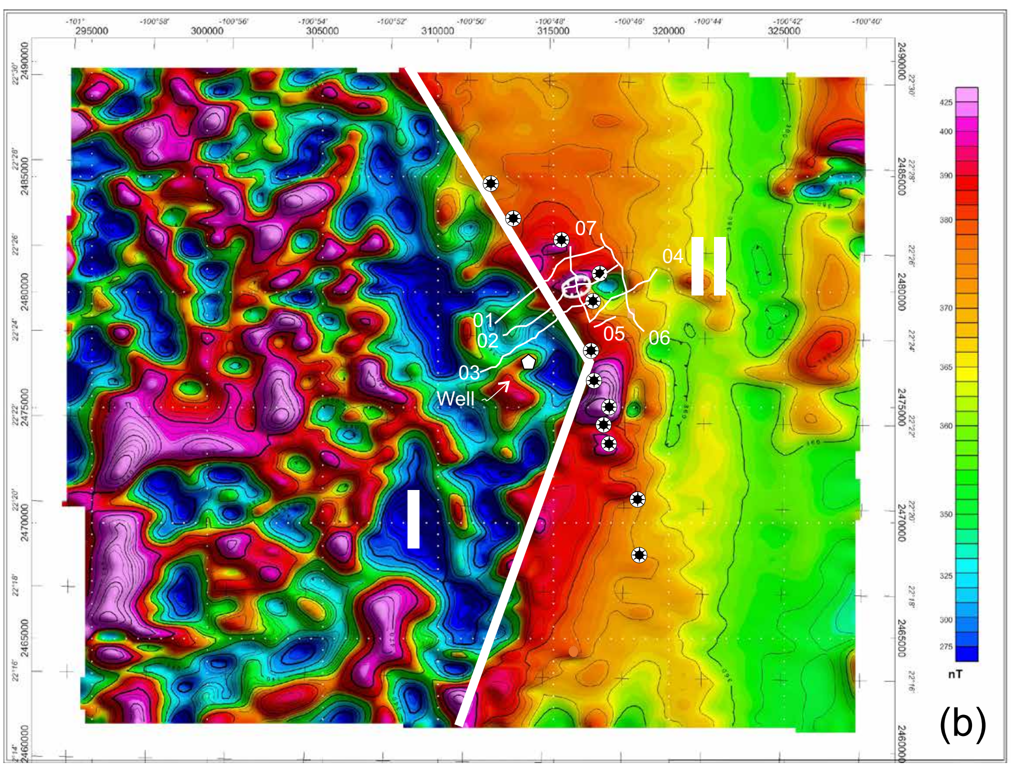

Figure 24. Aeromagnetic maps of the Villa Hidalgo 1:50,000 quadrangle (see location in Figure 5). (a) Magnetic field after subtraction of the corresponding IGRF values for 2000. (b) The data was reduced to the pole. The map also shows the location of the known cinder cones, maars and intraplate type lava flows, as well as sections measured in the field; these are labeled 01-07. The heavy white line represents the approximate limit between the two regional magnetic domains discussed in the text. South of Joya Honda (white ellipse in Figure 9a), within domain I, a water well cut 87m of mid-Tertiary felsic volcanic rocks which were buried under 90 m of unconsolidated granular materials. Thus, domain I owes its characteristics to the presence of mid-Tertiary volcanic rocks.

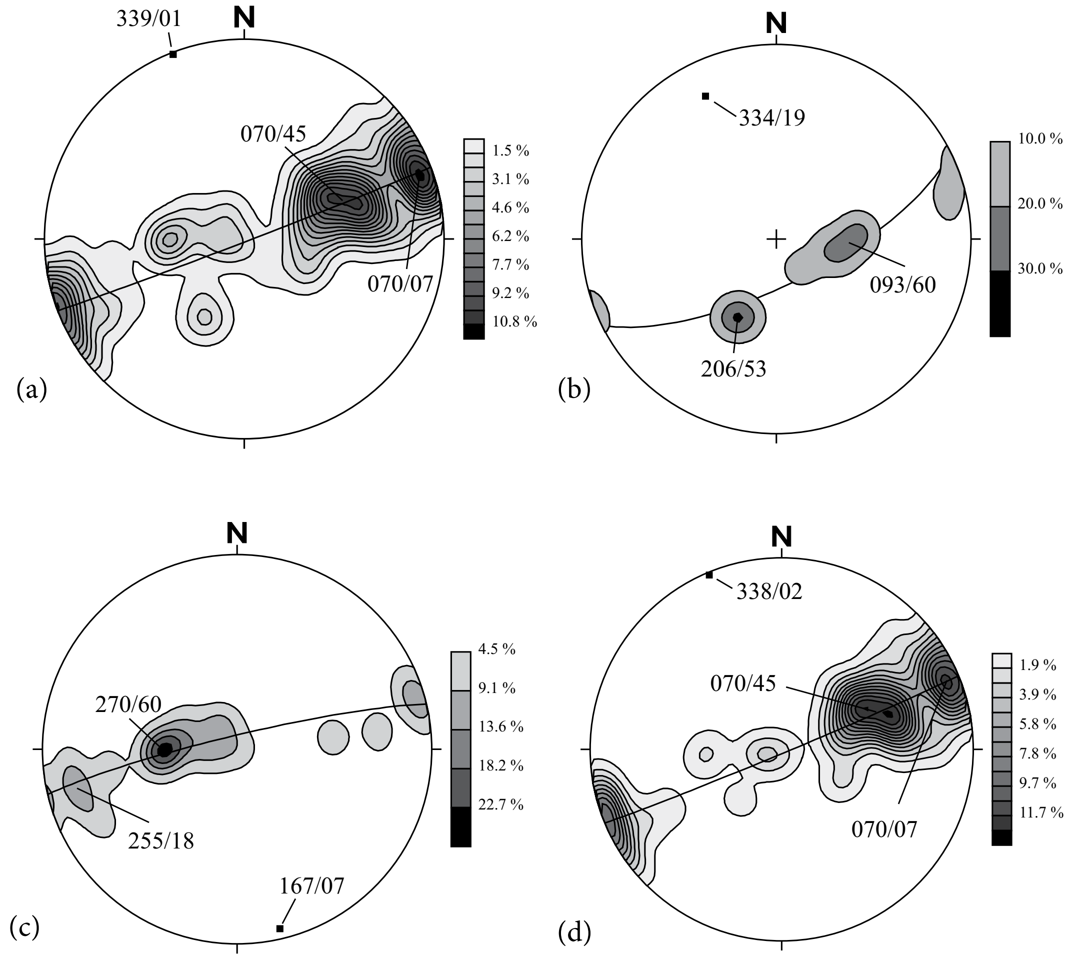

Figure 25. Contoured plots of poles to bedding projected into the lower hemisphere of an equal area net. (a) Data collected in the limestone exposed along the southern rim of the Joya Honda maar (n=130), (b) and (c) detailed measurements in second order folds exposed in the southern rim of the maar (n=10 and n=22, respectively), (d) Same as plot (a) after filtering out the data corresponding to obvious second order folds (Aranda-Gómez *et al.*, 2000).

the blast damage caused by the hydrovolcanic explosions was greater in the direction parallel to the major axis of the crater? Could these results be extended to other craters, such as Joya Prieta, which is also perpendicular to the local Laramide structure as shown by Aranda-Gómez *et al.* (2000)?

Recall the question raised in Stop 1.3 about the possibility that the SE flanks of Sierra El Coro and Sierra San Pedro are controlled by normal faults. Figure 24 is an aeromagnetic map of the Villa Hidalgo quadrangle (see location in Figure 5) and it shows two different aeromagnetic domains close to the Ventura volcanic lineament. West of the lineament is domain I characterized by wavelengths in the order of 500 m and series of highs and lows with superimposed high-frequency anomalies. East of the lineament, in domain II, the magnetic pattern has longer wavelengths (>2 km) and magnetic intensities between 320 and 380 nT. A visual comparison with the regional geologic map shows that domain I corresponds with outcrops of mid-Tertiary volcanic rocks and areas covered by alluvium, and domain II with areas where outcrop geology is dominated by Mesozoic carbonates. López-Loera *et al.* (2008) interpret the boundaries between the aeromagnetic domains as fault contacts. We note that the most remarkable xenolith localities, and the largest intraplate volcanoes are located at the place where these inferred faults intersect.

REFERENCES

AGI, 1974, Glossary of Geology, Falls Church VA, American Geophysical Institute, 805p.

Aranda-Gómez, J.J., 1982, Ultramafic and high grade metamorphic xenoliths from central Mexico [PhD thesis], Eugene, University of Oregon, 228p.

Aranda-Gómez, J.J., Dávila-Harris, P., Vassallo-Morales, L.F., Godchaux, M., Bonnichsen, B., Martínez-Reyes J., Aguirre-Díaz, G., y Ortega-Rivera, M.A., 2012, Geology and tectonics of the southeastern portion of the Sierra de Guanajuato: The Geological Society of America, Field Guide 25, 135-62.

Aranda-Gómez, J.J., Henry, C.D., Luhr, J.F., and

McDowell, F.W., 2003a, Cenozoic volcanic-tectonic development of northwestern Mexico—a transect across the Sierra Madre Occidental volcanic field and observations on extension-related magmatism in the southern Basin and Range and Gulf of California tectonic provinces, *in* Geologic transects across Cordilleran Mexico, Guidebook for the field trips of the 99th Geological Society of America Cordilleran Section Annual Meeting, Puerto Vallarta, Jalisco, Mexico, March 25-30, 2003: Mexico, D.F., Universidad Nacional Autónoma de México, Instituto de Geología, Publicación Especial 1, Field trip 5, p. 71–121

Aranda-Gómez, **J.J.,** Housh, T.B., Luhr, J.F., Becker, T., Solorio-Munguía, J.G, and Martínez, E., 2001, Timing of multiepisodic deformation based on the study of continental clastic deposits and volcanic rocks, east-central Chihuahua, México, GEOS, v.21, n. 3, p. 204.

Aranda-Gómez, J. J., and Luhr, J. F., 1993, Geology of the Joya Honda and Santo Domingo maars, San Luis Potosí, Mexico -A visit to the mantle and crustal xenolith localities in the Sierra Madre Terrane, *in* Ortega-Gutiérrrrez, F., Centeno-García, E., Morán-Zenteno, D. J., and Gómez-Caballero, A., eds., First circum-Pacific and circum-Atlantic Terrane Conference. Pre-Mesozoic basement of NE Mexico, crust and mantle xenoliths of central Mexico, and northern Guerrero terrane. Guidebook of field trip A: Guanajuato, Gto., Universidad Nacional Autónoma de México, Instituto de Geología, p. 10-35

Aranda-Gómez, J.J., Luhr, J.F., Housh, T.B., Connor, C.B., Becker, T., Henry, C.D., 2003b, Synextensional Plio-Pleistocene eruptive activity in the Camargo volcanic field, Chihuahua, México: Geological Society of America Bulletin, v. 115, n. 3, p. 298-313.

Aranda-Gómez, J.J., Luhr, J.F., Housh, T.B., Valdez-Moreno, G., and Chávez-Cabello, G., 2007, Late-Cenozoic intraplate-type volcanism in México: A review, in Alaniz-Álvarez, S.A. and Nieto-Samaniego, A.F. eds., Geology of México: Celebrating the Centenary of the Geological Society of México, Geological Society of America Special Paper 422, p. 93-128.

Aranda-Gómez, J.J. McDowell, F. W., 1998, Paleogene extension in the southern Basin and Range Province of México: Syndepositional tilting of Eocene red beds and Oligocene volcanic rocks in the Guanajuato mining district: International Geology Review, v.40, n.2, p.116-134

Aranda-Gómez, J.J., Torres-Hernández, J.R., Carrasco-Núñez, G., and Aguillón-Robles, A., 2000, Contrasting styles of Laramide folding across the west-central margin of the Cretaceous Valles-San Luis Potosí carbonate platform, Mexico, Revista Mexicana de Ciencias Geológicas, v. 17, n. 2, p. 97-111.

Aranda-Gómez, J.J., Molina-Garza, R.S., McDowell, F.W. Vassallo-Morales, L.F., Ortega-Rivera, M.A., Solorio-Mungía, J.G., and Aguillón-Robles, A., 2007, The relationships between volcanism and extension in the Mesa Central: the case of Pinos, Zacatecas, Mexico, Revista Mexicana de Ciencias Geológicas, v. 24, núm. 2, p. 216-233.

Aranda-Gómez, J.J., Luhr, J.F., and Pier, J., 1993, Geología de los volcanes cuaternarios portadores de xenolitos provenientes del manto y de la base de la corteza del Estado de San Luis Potosí, Instituto de Geología, UNAM, Boletín 106, p.1-22.

Aranda-Gómez, J.J., and Luhr, J.F., 1996, Origin of the Joya Honda maar, San Luis Potosí, México: Journal of Volcanology and Geothermal Research, 74, p. 1-18.

Aranda-Gómez, J.J., Luhr, J.F., and Pier, J.G., 1992, The La Breña and El Jagüey Maar Complex,, Durango, México. Part. I. Geological evolution: Bull. Volcanol., 54, p.393-404.

Basu, A. R. 1977. Olivine-spinel equilibria in lherzolite xenoliths from San Quintín, Baja California. Earth and Planetary Science Letters 33: 443-450.

Cantagrel, J.-M. and Robin, C. 1978. K-Ar dating on eastern mexican volcanic rocks- relations between the andesitic and the alkaline provinces. Journal of Volcanology and Geothermal Research 5: 99-114.

Carranza-Castañeda, O. *et al.*, 1994, Preliminary investigation of the geology of the northern San Miguel Allende area, northeastern Guanajuato, Mexico. Brigham Young Geology Studies 40:1-10.

Carranza-Castañeda, O. *et al.*, 2013, The early-late Hemphillian (Hh2) faunal assemblage from Juchipila Basin, State of Zacatecas, México and its biostratigraphic correlation with other Hemphillian faunas in central Mexico: Contributions in Science and Science Series of the Natural History Museum Los Angeles County, 521:13-49.

Carrillo-Bravo, J., 1971, La Plataforma Valles-San Luis Potosí, Boletín de la Asociación Mexicana de Geólogos Petroleros, v.23, n.1-6, p. 1-102).

Dávalos-Elizondo, M. G., Aranda-Gómez, J. J. *et al.*, 2011, Metasomatismo modal en peridotitas del manto provenientes del campo volcánico de Santo Domingo, San Luis Potosí, México, GEOS, v. 31 n. 1, p.68.

Dávila-Harris, P, 2003, Historia eruptiva del cráter La Joyuela, San Luis Potosí. B.S Thesis, Facultad de Ingeniería, Universidad Autónoma de San Luis Potosí. 110P.

de Cserna, Z. d., 1969, The “Alpine Basin and Range Province” of north-central Chihuahua, *in*

Cordoba, D. A., Wenegerd, S.A., Shoemaker, J., ed., Guidebook of the Border region; New Mexico Geological Society, 20th Field Conference, p. 66-67.

Díaz-Padilla, G. *et al.*, 2011, Mapeo del índice de aridez y su distribución poblacional en México, Revista Chapingo, v.17, p. 267-275.

Ferrari, L., M. Valencia-Moreno, *et al.*, 2007, Magmatism and tectonics of the Sierra Madre Occidental and its relation with the evolution of teh western margin of North America, *in* Alaniz-Alvarez, S. A .and Nieto-Samaniego. A. F. eds., Geology of México: Celebrating the Centenary of the Geological Society of México, Boulder CO, The Geological Society of America, Special Paper 422, p. 1-39.

Fisher, R.V. and Waters, A.C., 1970, Base-surge bed forms in maar volcanoes, American Journal of Science 268, 157-180.

Gross, W.H. 1975. New ore discovery and source of silver-gold veins, Guanajuato, Mexico, Economic Geology, v. 70, n. 7, p. 1175-1189.

Guzmán, E.J. and de Cserna, Z., 1963, Tectonic history of Mexico, in Childs, O.E. and Beebe, W.B., Backbone of the Americas: Am. Assoc. Pet. Geol. Memoir 2, p. 115-120.

Henry, C.D. and Aranda-Gómez, J.J. 1992. The real southern Basin and Range: Mid- to late-Cenozoic extension in Mexico. Geology 20:701-704.

Henry, C.D. and Aranda-Gómez, J.J. 2000, Plate interactions control middle-late Miocene proto-Gulf and Basin and Range extension in the southern Basin and Range. Tectonophysics 318: 1-26.

James, E.W and Henry, C.D. 1991, Compositional changes in Trans-Pecos Texas magmatism coincident with Cenozoic stress realignment: Journal of Geophysical Research, 96, 13561-13575

Labarthe-Hernández, G., 1978, Algunos xalapascos en el Estado de San Luis Potosí, Universidad Autónoma de San Luis Potosí, Instituto de Geología y Metalurgia, Folleto técnico 58, 17pp.

Labarthe-Hernández, G., Tristán, M., and Aranda-Gómez, J.J., 1982, Revisión estratigráfica del Cenozoico de la parte central del Estado de San Luis Potosí: Folleto técnico Instituto de Geología y Metalurgia, v.85, 208p.

López-Loera, H., Aranda-Gómez, J.J., Arzate-Flores, J.A., and Molina-Garza, R.S., 2008, Geophysical surveys of the Joya Honda Maar (México) and surroundings; volcanic implications: Journal of Volcanology and Geothermal Research, v. 170, p. 135-152.

Lorenz, V., 1986, On the growth of maar and diatremes and its relevance to the formation of tuff rings, Bulletin of Volcanology, v. 48, p. 265-274.

Lorenz, V. and Kurszlaukis, S., 2007, Root zone processes in the phreatomagmatic pipe emplacement model and consequences for the evolution of maar-diatreme volcanoes, Journal of Volcanology and Geothermal Research, v. 159, n. 1-3, p. 4-32.

Luhr, J.F., Aranda-Gómez, J.J., and Pier, J.G., 1989, Spinel- lherzolite-bearing, quaternary volcanic centers in San Luis Potosí, México. I. Geology, Mineralogy, and Petrology, Journal of Geophysical Research, 94, p.7916- 7940.

Luhr, J.F., Aranda-Gómez, J.J., and Housh, T.B., 1995b, The San Quintín Volcanic Field, Baja California Norte, México: Geology, Petrology and Geochemistry, Journal of Geophysical Research, v.100, n. B7, p.10353-10380.

Luhr, J.F., Pier, J.G., Aranda-Gómez, J.J., and Podosek, F.A., 1995a, Crustal contamination in early Basin and Range hawaiites of the Los Encinos Volcanic Field, central Mexico, Contributions to Mineralogy and Petrology, 118, p.321-339.

Luhr, J. F. and Aranda-Gómez, J. J., 1997, Mexican peridotite xenoliths and tectonic terranes: correlations among vent location, texture, temperature, pressure, and oxygen fugacity, Journal of Petrology, v. 38, n.8, p.1075-1112.

Luhr, J. F., Henry, C. D., Housh, T. B., Aranda-Gómez, J. J., and McIntosh, W. C., 2001, Early extension and associated mafic alkalic volcanism from the southern Basin and Range Province: Geology and petrology of the Rodeo and Nazas volcanic fields, Durango (Mexico), Geological Society of America Bulletin, v. 113, n. 6, p. 760-773.

Luhr, J.F., Kimberly, P., Siebert, L, Aranda-Gómez, J.J., Housh, T.B., and Kysar M. G., 2006, México's Quaternary volcanic rocks: Insights from the MEXPET petrological and geochemical database, *in* Siebe, C., Macías, J.L., and Aguirre-Díaz, G.J., eds., Neogene-Quaternary continental margin volcanism: A perspective from Mexico: Geological Society of America Special Paper 402, p. 1–44.

Mercier, J. C. C. and Nicolas, A., 1975, Textures and Fabrics of Upper-Mantle Peridotites as Illustrated by Xenoliths from Basalts, Journal of Petrrology, v. 16, n. 2, p. 454-487.

Muñoz-Saldúa, R. and Soto-Regalado, D. 1977, Cartografía geológica Hoja Pozas de Santa Ana, S.L.P., Universidad Autónoma de San Luis Potosí, Instituto de Geología y Metalurgia, Folleto técnico 55, 15p.

Pier, J.G., Luhr, J.F., Podosek, F.A. and Aranda-Gómez, J.J., 1992, The La Breña-El Jagüey maar complex, Durango, Mexico: II. Petrology and geochemistry, Bulletin of Volcanology, v. 54, p. 405-428.

Pier, J.G., Podosek, F., Luhr, J.F., Brannon, J. And Aranda-Gómez, J.J., 1989, Spinel-lherzolite-bearing, Quaternary volcanic centers in San

Luis Potosí, México. II. Sr and Nd isotopic systematics, Journal of Geophysical Research, v.94, p.7941-7951.

Pettus, D. S. (1979). Ultramafic xenoliths from Llera de Canales, Tamaulipas, Mexico. Department of Geology. Houston, TX, University of Houston, 65p.

Ruíz, J., Ortega-Gutiérrez, F., and Essene, E.J., 1983, Geochemical and petrographic characteristics of inclusions in Cenozoic alkalic basalts from central Mexico: EOS Transactions of the American Geophysical Union, 64, p. 343.

Smith, R.D. 1993. The Agua de Mayo mid-Cenozoic volcanic group and related xenoliths from La Olivina, southeast Chihuahua, Mexico, Msc thesis, University of California Santa Cruz, 112p.

Stewart, J.H., Anderson, R.E., Aranda-Gómez, J.J., *et al.*, 1998, Map showing Cenozoic tilt domains and associated structural features, western North America, in J. E. Faulds, and J. H. Stewart, eds., Accomodation zones and transfer zones: The regional segmentation of the Basin and Range Province, Boulder, Colorado, Geological Society of America, p. Plate 1.

Suter, M., 1991, State of stress and active deformation in Mexico and western Central America, in Slemmons, D.B., Engdahl, E.R., Zoback, M.D., and Blackwell, D.D. eds, Neotectonics of North America.Geological Society of America, Boulder CO, p. 401-421

Treviño-Cázares, A. *et al.*, 2005. Mantle xenoliths and their host magmas in the Eastern Alkaline Province, Northeast Mexico. International Geology Review 47: 1260-1286.

Tristán-González, M., 1986. Estratigrafía y tectónica del graben de Villa de Reyes, en los estados de San Luis Potosí y Guanajuato. Folleto Técnico del Instituto de Geología y Metalurgia de la Universidad Autónoma de San Luis Potosí n. 107, 1-91.

Tristán-González, M. *et al.*, 2009. Geocronología y distribución espacial del vulcanismo en el Campo Volcánico de San Luis Potosí. Boletín de la Sociedad Geológica Mexicana 61(3): 287-303.

Wohletz, K. H. and Sheridan, M. F., 1983, Hydrovolcanic explosions: II. Evolution of basaltic tuff rings and tuff cones, American Journal of Science, v. 283, p. 385-413.

§

We acknowledge our sponsors for their support to this meeting:

Commission on Monogenetic Volcanism

CVL IAVCEI Commission on Volcanic Lakes

CVS Commission on Volcanogenic Sediments

Centro de Geociencias

Coordinación de la Investigación Científica

CONACYT

IAVCEI

IAS

CONCYTEQ

CAC Centro Académico Cultural

Universidad Nacional Autónoma de México

Centro de Geociencias
Universidad Nacional Autónoma de México
Querétaro, Mexico, November 2014

http://maar2014.geociencias.unam.mx